Proceedings of JCF16, **16-14**, 158 – 198 (2016), ISSN 2187-2260

The Cold Fusion Phenomenon and Neutrons in Solids*

Hideo Kozima and Kaori Kaki[+]
Cold Fusion Research Laboratory
http://www.geocities.jp/hjrfq930/
597-16 Yatsu, Aoi, Shizuoka, 421-1202 Japan
[+]Shizuoka University, 836 Oya, Suruga, Shizuoka, 422-8529 Japan

Abstract

A phenomenological approach, the trapped neutron catalyzed fusion model (TNCF model) where assumed existence of thermal neutrons in CF materials, to the science of the cold fusion phenomenon (CFP) is reviewed with attention to the behavior of neutrons in solids, especially in CF materials composed of the superlattice of a host sublattice and a hydrogen sublattice. The success of the TNCF model to give a unified explanation of widely dispersed experimental data obtained in the CFP suggests reality of the fundamental premise of the model, existence of the trapped neutrons in CF materials. Taking this clue as a hint showing a possible existence of neutrons in such specific solids as CF materials, in which there is a superlattice composed of host and hydrogen isotope sublattices, we have tried to find out a new state of neutrons in them not noticed in solid state physics and in nuclear physics by now. A possible quantum mechanical formation of neutron energy bands in CF materials is investigated using techniques developed in the electron energy bands in solids.

1. Introduction

The cold fusion phenomenon (CFP) was discovered by Fleischmann et al. in 1989 at least one of its phases related to the excess energy [Fleischmann 1989]. Another phase of the phenomenon, emission of neutrons, was confirmed by Jones et al. almost at the same time [Jones 1989]. However, these data were not accepted by scientific world at that time due to the following reasons.

The pioneers of this field cited above had been eager to find out a clue of nuclear fusion reactions between two deuterons in solid lattices containing a lot of deuterium, a hydrogen isotope, assisted by the lattice environment irrespective of tiny energies of deuterons, other atoms and ions in the system at the near room-temperature.

In general, a nuclear reaction between two nuclides ${}^{A}_{Z}\mathrm{X}$ and ${}^{A'}_{Z'}\mathrm{X'}$ is written down as follows;

$$ {}^{A}_{Z}\mathrm{X} + {}^{A'}_{Z'}\mathrm{X'} \rightarrow {}^{A''}_{Z''}\mathrm{X''} + {}^{A'''}_{Z'''}\mathrm{X'''} + Q, \qquad (1.1) $$

with Q ~ a few MeV. Despite of the findings by the above pioneers, almost all scientists working in the nuclear physics did not accept the idea of the nuclear fusion reactions in solid relying on the following three main reasons;

(1) The probability of the reaction (1.1) depends exponentially on the mutual energy ε of the initial particles as follows;

$$ P \sim C(\sqrt{\mu}/\hbar) \exp[-\int\sqrt{(V(x) - \varepsilon)}\, \mathrm{d}x], \qquad (1.2) $$

where $V(x)$ is the barrier potential between the two particles, μ is the reduced mass and C a constant. For the two charged nuclei, the potential $V(x)$ is very high and it is necessary to have several MeV for the energy ε for a measurable number of the reaction (1.1). We have desperately small values of P for *d-d* fusion reactions when deuterons are in Pd lattice forming a palladium deuteride PdD at room-temperature.

(2) The liberated energy Q in such a usual reactions as (1.1) has very high energy compared to the thermal energy of the room-temperature solids of about 0.025 eV or 25 meV;

$$ Q \sim \text{about a few MeV.} \qquad (1.3) $$

Therefore, the energy Q should be detected as a special physical quantity in the lattice; e.g. as high energy particles or local radiation damages.

(3) As we have known well, a physical process should be reproducible strictly in simple systems and statistically in systems with stochastic processes. Unfortunately, we have failed to show the strict or even statistical reproducibility for observables in the cold fusion phenomenon.

These three main problematic obstacles we had in this field have made the facts measured by CF researchers forlorn by scientists in the established fields of science. There have been proposed many mechanisms to overcome the three obstacles by tricks and devices not noticed in the past by scientists in other field. Our trial, only one successful approach from our point of view, to overcome them and to give a unified and consistent explanation of the cold fusion phenomenon is given in Section 2.

It is necessary to give a word on the name “cold fusion” used for more than 20 years since 1989. The name has been used by pioneers of this field based on their expectation that such a reaction (1.1) occurs between two deuterons in specific CF materials (PdD_x and TiD_x). We have a research field, solid state-nuclear physics or condensed matter nuclear science, where the nuclear force between nucleons (protons and neutrons) influence the physical processes occurring in solids or condensed matters. Therefore, the so-called cold fusion belongs to the solid state-nuclear physics and we can use the

name “solid state-nuclear physics” to express the “cold fusion.” It is, however, more convenient to distinguish the “cold fusion” where occur nuclear reactions, and therefore nuclear transmutations, from other events in the “solid state-nuclear physics” where had not been observed nuclear reactions until 1989. This is the reason we have used the name “cold fusion phenomenon” to express the phenomenon in the solid state-nuclear physics where occur nuclear reactions.

As has been shown in our books and papers published since 1994 [Kozima 1994, 1998a, 2006, 2009b, 2014a] and in our papers in the Series “*From the History of CF Research*” [Kozima 2015], our phenomenological approach using the TNCF model (Trapped Neutron Catalyzed Fusion model) is successful to give a unified understanding of the CFP. In other words, our trial to construct the *Science of the Cold Fusion Phenomenon (CFP)* arranging experimental facts in a proper position according to this model has been useful and successful to explain various complicated experimental facts in the CFP systematically to understand them scientifically. However, it should be remembered that the premises composing the model have not necessarily been elucidated quantum mechanically.

Generally speaking, the proverb “You cannot see the wood for the trees” is applicable to the many works on the cold fusion phenomenon done in these more than 25 years; picking up only a specific feature of the CFP and trying to explain it with a sophisticated model elaborating complicated calculation. Therefore, the success of the phenomenological TNCF model in explanation of overall features of the CFP is outstanding and it is necessary to investigate and contemplate the basis of the model from the modern microscopic point of view.

After the successful explanation of experimental facts in the CFP summarized in the book published in 1998 [Kozima 1998a], we have developed a quantum mechanical explanation of the premises presumed in the TNCF model [Kozima 2006, 2014a], especially the existence of the trapped neutrons in such CF materials as NiH_x, PdD_x, carbon graphite, cross-linked polyethylene (XLPE). In the investigation, we noticed that there are new knowledges of nuclear and solid state physics in their frontiers developing rapidly.

Therefore, we have to say that the physics of CF materials is in its infantile stage where we define the CF materials as the system composed of lattice nuclei and hydrogen isotopes, such as NiH_x, PdD_x, CH_x, etc. and the host nuclei and hydrogen isotopes are interacting mainly through the nuclear force (the central nucleon-nucleon interaction). Experimental facts of the CFP and the diffusion characteristics of hydrogen in transition metals might be subtle signals of the new states in CF materials as we show

in this paper. Theoretically, the new knowledge of the exotic nuclei on one hand and the characteristics of transition-metal hydrates on the other are the hint to cultivate the physics of CF materials.

It is interesting to recollect the frontiers of nuclear physics at 1960s when one of the authors (H.K.) was a graduate student. The late Professor Toshinosuke Muto (1904 – 1973), Tokyo University, his instructor at the graduate course, used to say at seminars on nuclear physics that there are many interesting research themes in the low energy region (the energy regions below a few MeV) of nuclear physics while the high-energy region (more than 100 MeV) was attracting many researchers at that time. His comment on the importance of low and medium energy nuclear physics at that time has shown its correctness when we notice the recent vivid researches in ultra-low energy neutrons and exotic nuclei in terms of the shell model (cf. Sec. 4). A new trend of recent researches in nuclear physics is expressed in the following sentence by Sahin et al.: "*The interplay among central, spin-orbit, and tensor components of the effective nucleon-nucleon interaction can shift effective single-particle energies relative to each other as protons and neutrons fill certain orbitals near the Fermi surface in nuclei with large neutron excess.*" [Sahin 2015]

The exotic nuclei with a large excess of neutron numbers such as $^{11}_{3}$Li and $^{12}_{4}$Be might be the signal of such exotic nuclei as $^{A}_{6}$C, $^{A}_{28}$Ni, and $^{A}_{46}$Pd with the nucleon numbers *A's* exceeding largely the values of ordinary isotopes participating in the CFP [Kozima 2014b]. In reality, recent works on the exotic nuclei have confirmed existence of $^{32}_{12}$Mg [Utsuno 2014], $^{42}_{14}$Si [Stroberg 2014], $^{69}_{29}$Cu [Morfouace 2014], $^{73}_{29}$Cu [Sahin 2015], $^{92}_{42}$Mo [Sharp 2013] which were investigated in relation to the bases of the shell model of nucleus as discussed in Section 4.

Therefore, it is possible to consider that the investigation of neutron bands in CF materials developed in this paper is a tentative model for neutron physics in solids corresponding to the liquid-drop model of nuclei for nuclear reactions in the early stage of nuclear physics.

2. Phenomenological Approach to the Cold Fusion Phenomenon – the Trapped Neutron Catalyzed Fusion Model

The Trapped Neutron Catalyzed Fusion model (TNCF model) was proposed at ICCF4 held at Hawaii, USA on 1994 [Kozima 1994]. The model was a phenomenological approach based on experimental facts obtained in these five years after the declaration of the discovery of the CFP in 1989 by Fleischmann et al. [Fleischmann 1989]. These experimental facts obtained by the time were too

complicated to understand by the sciences on principles established in 20th century and were also looked upon with deep suspicion.

In relation to the three main obstacles explained in Section 1, we can give a brief idea of our model to overcome them.

(1) To avoid the difficulty of the Coulomb barrier penetration (cf. Eq. (1.2)), we have taken up neutrons which have no problem to reach a target nuclide [Kozima 1994, 1998a, 2006].

(2) The liberated energy Q (1.3) in the Eq. (1.1) is supposed to be shared by lattice nuclei [Kozima 1998a, 2006, 2014a].

(3) The problem of the reproducibility is resolved by the idea of complexity, such as self-organization, inherent in the formation of such CF materials as PdD_x, NiH_x, H_xC_6, etc. where occurs the CFP [Kozima 2012, 2013, 2014a].

We have given unified explanation of various experimental data sets obtained in this field in these more than 25 years [Kozima 1998a, 2006, 2012, 2013, 2014a]; It should be mentioned that the explanation in the initial stage of the TNCF model applied to the CFP has been done using only absorption of a single neutron by relevant nuclides in the CF materials [Kozima 1998a]. To explain experimental data of nuclear transmutations with large changes of proton and nucleon numbers, Z and A, it was necessary to introduce an idea of neutron drops suggested by the work by Negele et al. on the neutron star matter [Negele 1973] as explained below.

The success in the explanation of experimental data by our model at this stage substantiates the premises of the TNCF model and the recent works including this paper have been elaborated to explain the premises from fundamental bases of quantum mechanics and nonlinear dynamics.

In the process of explanation of variety of experimental data obtained in the CFP, there happened a chance to have connection with the neutron star matter. There occurred a necessity to explain nuclear transmutations with larger changes of proton and nucleon numbers, Z and A, more than two. To treat these cases, we have taken into our model a possibility of absorption of a neutron cluster ${}^{A}_{Z}\delta$ or ${}^{A}_{Z}\Delta$ with $A \geq 2$ and $Z \geq 2$ composed of Z protons and $A - Z$ neutrons. We will call them a "neutron drop" hereafter [Kozima 2006]. The idea of the neutron drop was suggested by the work by Negele and Vautherin [Negele 1973] for the neutron star matter; they had shown that there appears a lattice of the neutron drops ${}^{A}_{Z}\Delta$ with a lattice constant a by self-organization. The lattice constant a and the A/Z ratio of the neutron drop ${}^{A}_{Z}\Delta$ depends on the average neutron density N_n of the neutron star matter.

Then, we can write down such reactions with large changes of proton or nucleon

numbers as follows;

$$ {}^{A}_{Z}\mathrm{X} + {}^{A'}_{Z'}\Delta \rightarrow {}^{A''}_{Z''}\mathrm{X'}^{*}\ (Z + Z' = Z'',\ A + A' = A'') \qquad (2.1) $$

with possible decay processes of the resultant nuclide ${}^{A''}_{Z''}\mathrm{X'}^{*}$. (We dare use the notation ${}^{A}_{Z}\mathrm{X}$ despite the duplication of the proton number Z and the elemental symbol X to make easy the arithmetic in the nuclear transmutations often appear in the CFP). The application of the reactions of these types is given in our explanation of many nuclear transmutations in our book and papers [Kozima 2006, 2008, 2010, 2014c].

One of the most fundamental premises of the model is the existence of the so-called "trapped neutrons" with thermal energy which interact with nuclei at irregular positions and foreign nuclei in CF materials. Even if the model has given qualitative or even semi-quantitative explanations for the experimental facts [Kozima 1998a (Sec. 11), 2006 (Sec. 3.2)], the reality of the assumed existence of the trapped neutrons has been questionable.

To investigate the reality of the trapped neutrons in CF materials, we have examined behavior of neutrons in solids. The first idea of possible formation of neutron bands in solids is suggested in analogy to the electron bands formation based on the quasi-free electron approximation [Kozima 1998a] (cf. Appendix A1). In relation to this mechanism, several papers on the quasi-bound states of neutrons in solids are cited already in our books. The paper by Hino et al. [Hino 1998] used Fabry-Perot magnetic thin film resonator to trap neutrons in quasi-bound states. The more extensive references will be given in the next section.

As the second mechanism of the neutron band formation, we have developed a possible interaction of lattice nuclei mediated by occluded hydrogen isotopes [Kozima 2004a, 2004b]. The interaction of neutrons in different lattice nuclei results in band formation by the mechanism similar to the tight-binding approximation of the electron band (cf. Appendix A2).

The fundamental step to the neutron band formation by the former quasi-free approximation is, in reality, worked out in several experiments using ultra-cold neurons (UCN's) as surveyed in the next section 3.1. The justification of the latter tight-bound approximation took place its first step in our works using a possible interaction of lattice nuclei mediated by occluded hydrogen isotopes [Kozima 2004a, 2004b, 2006 (Sec. 3.5)]. Extension of our treatment will be given in Section 5.2.

3. Band Structure of Electron Energy in Solids

The energy spectrum of a microscopic object is very different from that of a macroscopic object as noticed in the first stage of the discovery of quantum nature of

matter. Rather, the characteristic of the energy spectrum of a harmonic oscillator gave a chance to notice the discontinuous property of microscopic objects in the first year of the 20th century.

It is well known that electrons in crystals have their energies arranged as energy bands composed of allowed bands and forbidden bands. The mutual relation of the allowed and forbidden bands and the number of electrons in them determine physical natures of the crystals. The band structure of a crystal has close relation with the energy levels of composite atoms of the crystal and is investigated from several appropriate points of view related closely to the nature of the atoms.

There are two contrasting approaches to look the nature of the energy band; the quasi-free particle approach and the tight-binding particle approach as reviewed in Appendix of this paper. The former approach treats the electron energy level in the crystal as a level of an electron state in free space, i.e. a plane wave, perturbed by atomic potentials, as reviewed in Appendix A1. The latter approach treats the electron energy level in the crystal as a linear combination of electron states in the atoms composing the crystal and the electron energy band reflects strongly the nature of the energy in the atom as reviewed in Appendix A2.

These treatments of the electron energy bands are similarly applicable to the case of neutrons in solids as discussed in Section 5 in an analogical way to the electron energy bands.

4. Neutrons in a Nucleus

After the discovery of the neutron in 1932 by J. Chadwick [Kozima 2006 (Appendix D)], it has been concluded that a nucleus is composed of neutrons and protons different from the idea that a nucleus is composed of electrons and protons. Many properties of the nucleus had been investigated using high energy particles to penetrate the Coulomb barrier guarding the nuclei from approach of any charged particle [Blatt 1954] instead of neutrons which was out of use at first.

4.1. Single Neutron States in Ordinary Nuclei

It was a surprise of researchers in 1940's to know that nuclei show a single particle characteristic even if there are many evidences showing events explained by collective particle models such as the liquid drop model proposed by N. Bohr [Bohr 1937]. This feature of the nuclear properties was explained by the characteristics of the nuclear force with short-range, independent of nucleon charge and saturation property. The limited applicability of these characteristics deduced from experimental facts in

ordinary nuclei at stable states in free space have recognized gradually with progress of researches to nuclei in different situations as explained in this section.

4.1a Classical Approach

In the discussion of the bases of the TNCF model for the CFP, we have sometimes assumed the neutron states in lattice nuclei (e.g. Pd, Ni and Ti) are independent of the neutron number of isotopes of these nuclei. This assumption has its basis on the following discussion of the energy levels at higher levels.

Because the higher energy levels of nucleons in a nucleus are not much affected by addition of a neutron to the nucleus as discussed by Blatt and Weisscopf as cited below, the neutron states at zero-energy level in the lattice nuclei Ni (or Pd) are assumed to be the same ones independent of the number of neutrons in the Ni isotopes ${}^{A}_{28}\mathrm{Ni}$ (A = 58 – 64) (or Pd isotopes ${}^{A}_{46}\mathrm{Pd}$ (A = 102 – 110)).

"*In this argument we have assumed that only the lowest, or the lowest few, levels of a given nucleus are affected by the "spell" of the magic numbers. The higher levels are, assumed to be unchanged, i.e., their absolute energies are not lowered appreciably. The evidence from the neutron capture cross sections and from several other sources supports this qualitative picture*." [Blatt 1954 (p. 765)]

4.1b Modern View

The progress of investigation on the nuclear structure has revealed importance of single particle behavior of nucleons in a nucleus. An example of this tendency is expressed by Caurier in the abstract of their paper "The shell model as a unified view of nuclear structure" appeared in *Rev. Mod. Physics* (2005) [Caurier 2005];

"*The last decade has witnessed both quantitative and qualitative progress in shell-model studies, which have resulted in remarkable gains in our understanding of the structure of the nucleus. Indeed, it is now possible to diagonalize matrices in determinantal spaces of dimensionality up to 109 using the Lanczos tridiagonal construction, whose formal and numerical aspects are analyzed in this review.*

- - - - - - - - - - - - - - - - -

This combination appears to solve a number of hitherto puzzling problems. The present review concentrates on those results which illustrate the global features of the approach: the universality of the effective interaction and the capacity of the shell model to describe simultaneously all the manifestations of the nuclear dynamics, either single-particle or collective in nature. The review also treats in some detail the problems associated with rotational motion, the origin of quenching of the

Gamow-Teller transitions, double-b decays, the effect of isospin nonconserving nuclear forces, and the specificities of neutron-rich nuclei. Many other calculations—which appear to have "merely" spectroscopic interest—are touched upon briefly, although the authors are fully aware that much of the credibility of the shell model rests on them." [Caurier 2005]

Even in the nuclear physics in free space, the knowledge about the interaction of nucleons in an isolated nucleus has made progress by leaps and bounds in 50 years as the abstract cited above shows. Then, we can expect new features of nuclear physics about nuclei in interaction each other in such atmosphere as realized in CF materials as suggested by experimental facts introduced in Section 2.

4.1c Neutron States near the Evaporation Level

It is interesting to notice that there are neutron states at around the evaporation level in some stable nuclei as shown in Fig. 4.1 [Bohr 1969].

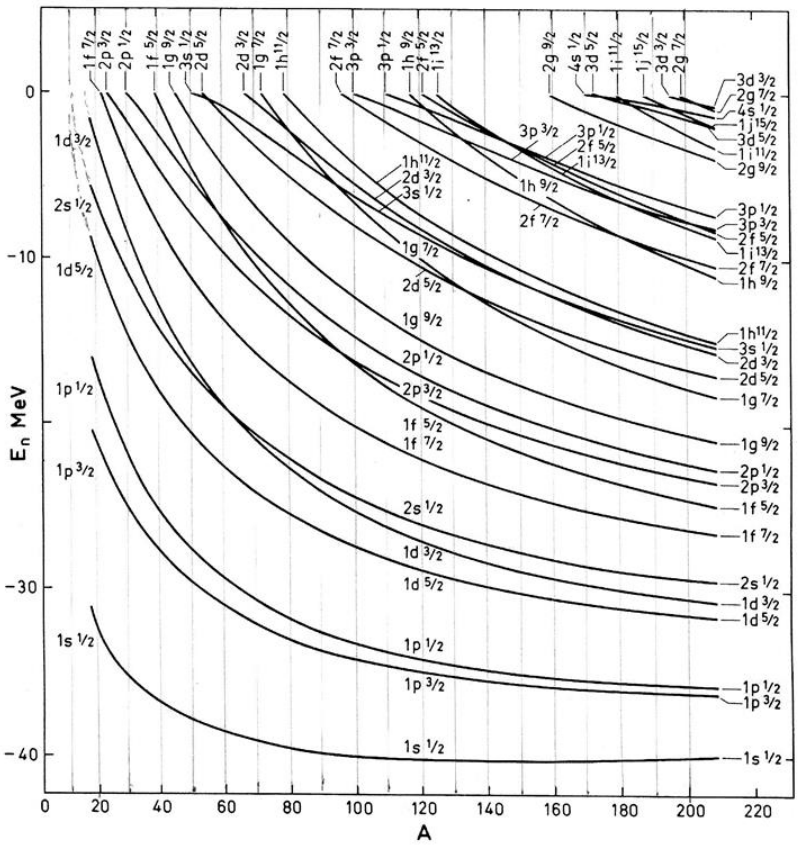

Fig. 4.1 Energies of neutron orbits in nuclei calculated by C.J. Veje [Bohr 1969]

We see in Fig. 4.1 that host elements of CF materials such as Ti, Ni, Pd and C have neutron orbits at around the evaporation level, i.e. at around $E_n \sim 0$ in this figure. This

characteristic of these nuclei may have close relation with the appearance of the CFP in such CF materials as TiD_x, NiH_x, PdD_x ($x \approx 1$) and the hydrogen graphite HC_x (x = 6 – 8) [Kozima 1998a, 2006, 2014a].

4.2 Neutron States in Exotic Nuclei

In our previous estimation of the neutron band [Kozima 2004a (Sec. 3), 2006 (Sec. 3.7)], we used a wavefunction $\psi_{\{n\}}(\boldsymbol{r} - \boldsymbol{a}_i)$ of a neutron state in a lattice nucleus at lattice point a_i, neglecting the fact that the lattice nuclei are one of several isotopes ${}^{A}_{28}Ni$ (A = 58 – 64 in NiH) or ${}^{A}_{46}Pd$ (A = 102 – 110 in PdD). In reality, the neutron $g_{9/2}$ orbital is filled gradually moving from ${}^{68}Ni$ to ${}^{78}Ni$.

Therefore, it might be permissible to use one of $g_{9/2}$ orbitals for the wavefunctions $\psi_{\{n\}}(\boldsymbol{r} - \boldsymbol{a}_i)$ of valence neutrons in ${}^{A}_{28}Ni$ in the calculation of the neutron band in NiH neglecting the possible linear combination of $g_{9/2}$ orbitals in the case of the CF material NiH_x. We have to recognize that our treatment of this problem is too oversimplified to ask any adequacy considering the complex nature of the nuclear interaction in nuclei with intermediate mass numbers.

The situation is rather complex as mentioned by Morfouace et al. and Sharp et al. as follows:

"*It is already known that magic numbers can change with the exoticity of the nuclei. An interesting case are the Ni isotopes (Z = 28). Moving from ${}^{68}Ni$ to ${}^{78}Ni$ the neutron $g_{9/2}$ orbital is filled. For example, the residual tensor interaction is supposed to be attractive for the $vg_{9/2}$—$\pi f_{5/2}$ and repulsive for the $vg_{9/2}$—$\pi f_{7/2i}$ configurations. With such an interaction we can see that the single-particle levels could evolve with the exoticity of the Ni isotopes. The three-body strength could also have a role in this mass region*." [Morfouace 2014]

"*Recent investigations into the structure of light nuclei have indicated dramatic changes in shell structure away from stability. The ordering of single-particle levels has been found to evolve as a function of proton-neutron ratio and even the locations of the gaps in levels that correspond to shell closures are found to alter. For example, the disappearance of the N = 20 magic number, and the emergence of a new shell gap at N = 16, have been observed in nuclei near the neutron drip line.*" [Sharp 2013]

Considering the complex physics of a single nucleus with medium number of nucleons as cited below from papers by Stroberg et al., Utsuno et al. and Sahin et al., we can guess the difficulty of our treatment of the CF-matter composed of neutrons in neutron bands and protons at interstices resulting as a consequence of the super-nuclear

interaction.

"*Shell evolution is studied in the neutron-rich silicon isotopes* ^{36,38,40}*Si using neutron single-particle strengths deduced from one-neutron knockout reactions. Configurations involving neutron excitations across the N = 20 and N = 28 shell gaps are quantified experimentally in these rare isotopes*." [Stroberg 2015]
"*In particular, the monopole components of effective interactions—the parts responsible for the* ***evolution of the shell structure****— are known to be subject to modification. This so-called shell evolution plays a decisive role in the structure of exotic nuclei, and has been attracting much interest in this field*." [Utsuno 2014]
"*Current nuclear structure studies are paying considerable attention to the search for anomalies in the shell structure of nuclei with large neutron-to-proton ratios. In these exotic regions of the nuclear chart, the separation between single-particle orbitals can be altered due to a changing ratio between* ***T*** *= I and T = 0 components of the nuclear force."* [Sahin 2015]
"The evolution of proton single-particle states as a function of neutron number for the chain of Ni isotopes between ^{68}*Ni and* ^{78}*Ni was investigated using the GXPFI residual interaction*." [Sahin 2015]

5. Neutrons in Solids

The neutron as an elementary particle has the wave-particle duality. The wave nature of the neutron is noticed from the first in relation to the interference with periodic arrangements of atoms and nuclei and applied to investigate material structure using the neutron scattering (e.g. [Shull 1947, 1956, Golub 1990]).

We have also noticed the wave nature of the neutron in relation to the TNCF model for the CFP and reviewed the nature of the neutron [Kozima 1998 (Sections 12.2 – 12.4)]. Even if our knowledge about interaction of neutrons with matter was scarce at that time, we have noticed the quasi-bound state of neutrons in solids (e.g. [Hino 1998]).

Looking for historical basis of the neutron-solid interaction, we have noticed profound researches originating from the work by E. Fermi in 1936 [Golub 1990, Fermi 1936]. There are many works on the neutron trapping in crystals due to the strong interaction in addition to that due to the magnetic interaction as surveyed in the next subsection lacking, however, the formation of the neutron band we have noticed in our previous works [Kozima 1998b, 2004, 2006] due, perhaps, to the finite life of free neutrons. We will give our opinion on this problem and our answer in this paper.

In the superlattice of a host sublattice and hydrogen sublattice (proton or deuteron sublattice) in CF materials, the interaction of neutrons in host nuclei and protons/deuterons at interstices should be treated as a many-body problem. In this paper, however, we have to consider the situation in a simplified manner as a problem of neutron band formation mediated by the proton/deuteron sublattice in CF materials, a specific array of host elements and hydrogen isotopes.

5.1 Quasi-free neutron approximation

The ultra-cold neutrons (UCN's) have been extensively investigated in these more than 30 years in relation to the researches of the fundamental nature of the neutron and also to its application [Golub 1990].

In the process of the investigation, the techniques to trap neutrons as long as possible in traps made of material surfaces and magnetic fields are developed.

The following figures give us a typical feature of neutron-matter interaction due to the strong interaction (nucleon-nucleon interaction) of a neutron and atomic nuclei in lattices [Scheckenhofer 1977, Steinhauser 1980].

Figures 5.1 – 5.3 show the neutron wave reflection characteristics described by a Schrödinger equation, the same to that for an electron wave explained in Section 3 and Appendix. (We can use parallelism for electrons and neutrons in this section.)

In Fig. 5.1, measured intensities reflected from a glass mirror (points) compared to theoretical curves are shown for (a) a step function, and (b) a smoothed step function for the wall scattering potential. In this figure, the abscissa "height of fall" (z) is used to designate the quasi-momentum k_z perpendicular to the potential variation (step function) according to the relation

$$k_z = (m/\hbar)\,(2gz)^{1/2}, \qquad (5.1.1)$$

where m is the neutron mass, g is the acceleration due to gravity.

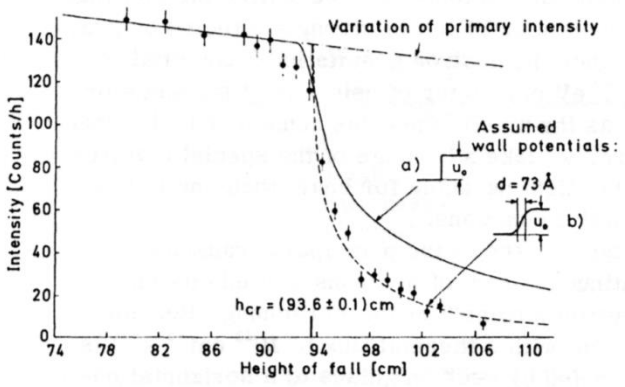

Fig. 5.1 Measured intensity reflected from a glass mirror (points) compared to theoretical curves for (a) a step function, and (b) a smoothed step function for the wall scattering potential. ---, calculation for mono-energetic neutrons; —, calculation for the instrumental resolution. Assumption (b) may be a model for a hydrogenous surface contamination. [Scheckenhofer 1977 (Fig. 3)]

In Fig. 5.2, reflected intensity measured as a function of the fall height is shown for a target potential depicted in the inserted figure with nominal layer thicknesses: Al (100 Å), Cu (240 Å), Al (860 Å), and Cu (240 Å). The abscissa "Fall Height" (z) in Figs. 5.2 and 5.3 corresponds to the "Height of Fall" in Fig. 5.1 and express the quasi-momentum k_z as explained above using the relation (5.1.1).

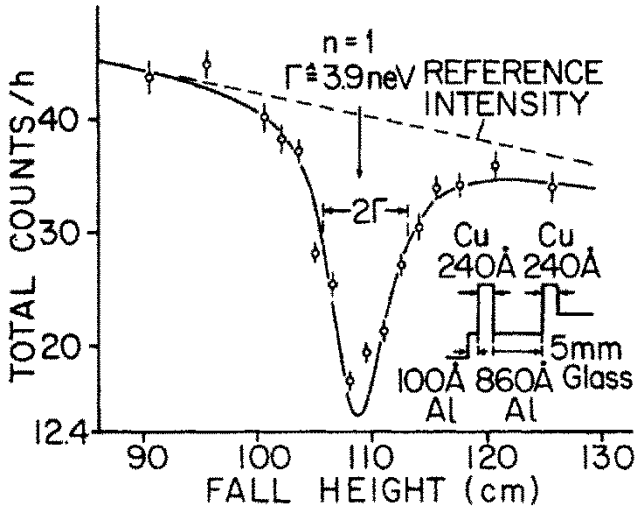

Fig. 5.2 Reflected intensity measured as a function of the fall height for a target with nominal layer thicknesses: Al (100 Å), Cu (240 Å), Al (860 Å), and Cu (240 Å). The substrate is glass. Potential functions representing these layers are shown in the inset. The intensity minimum at 108.5 cm corresponds to n = 1 (the second stationary state). The solid curve is an exact solution of the one-dimensional Schrödinger equation for the multistep potential representing the target and includes the instrumental resolution broadening. [Steinhauser 1980 (Fig. 2)]

In Fig. 5.3, transmission data is shown for a target with nominal layer thicknesses: Al (110 Å), Cu (180 Å), Al (1670 Å), Cu (180 Å), and Al (110 Å) as depicted in the inserted figure.

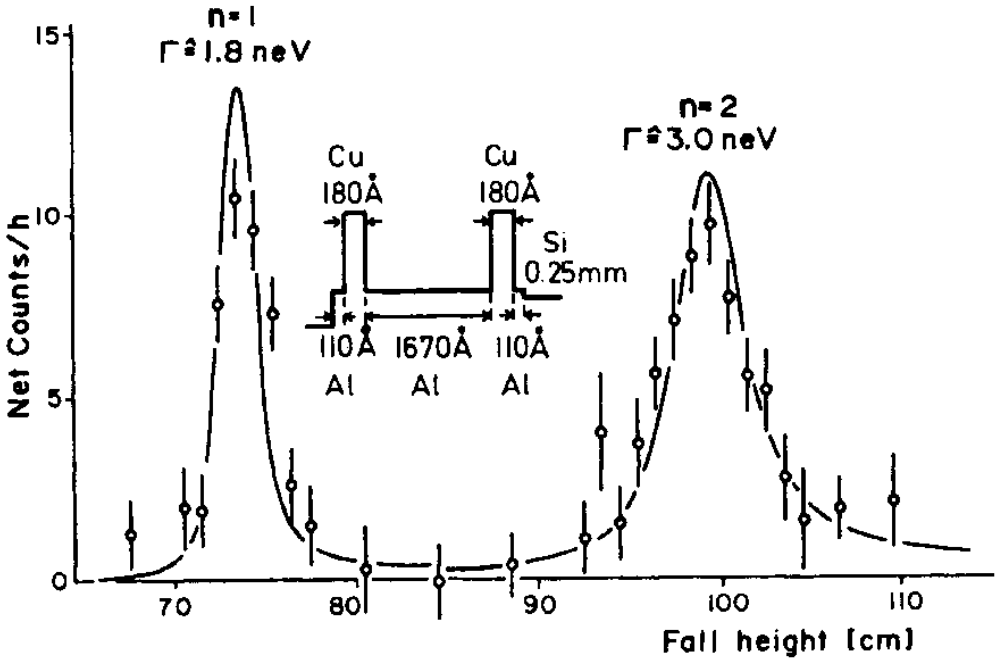

Fig. 5.3 Transmission data for a target with nominal layer thicknesses: Al (110 Å), Cu (180 Å), Al (1670 Å), Cu (180 Å), and Al (110 Å). The substrate is silicon of 0.25-mm thickness. The two resonances observed correspond to n = 1 and n = 2. The data are compared to the solid curve calculated for a multistep potential. [Steinhauser 1980 (Fig. 3)]

The data shown in Figs. 5.1 – 5.3 clearly express the expected wave nature of the neutron interacting with lattice nuclei through the nuclear force.

It is an obvious one-step from above investigations to such a neutron band structure as the electron band depicted in Fig. A3 in Appendix while the step is not traced due, perhaps, to the finite life time 889 ±3 s of the free neutron. However, it is easy to infer from the experimental data [Steinhauser 1980] obtained in the potential inserted into Fig. 5.3 that the neutron band is formed in such a potential as described in Fig. A2 for an electron.

Even if the neutron band is formed in a periodic potential as assumed in our previous works (e.g. [Kozima 1998a, 1998b]), the instability of the neutron due to the beta-decay accompanies also to the neutron in the band. So, the neutron bands are ineffective for any physics as far as there are no supplies of neutrons to the bands. However, the situation changes very much when there are neutron sources to supply enough neutrons to the energy band overwhelming the loss by decay. This situation may be a case in the CFP when there are neutron sources as discussed in our papers (e.g.

[Kozima 1998 (Sec. 8)])

It should be given an idea to stabilize the neutrons in the band based on the free-neutron approximation. The free neutrons interacting with lattice nuclei to form the neutron band might be able to stabilize against the beta-decay by the neutron-nuclear interaction if the interaction is strong enough to change the neutron from free to band states. This is only a speculation with a hope to facilitate the idea of the neutron band made of free neutrons for the CFP.

This problem of the neutron instability by the beta-decay, however, shows different feature in the case of the band discussed in the next subsection.

5.2 The Tight-binding Approximation for Neutron Band

Neutrons in a band formed of the tight-binding by neutron states in different lattice nuclei in a CF material have different characteristics from those in the band made of free neutron states as discussed in Sec. 5.1.

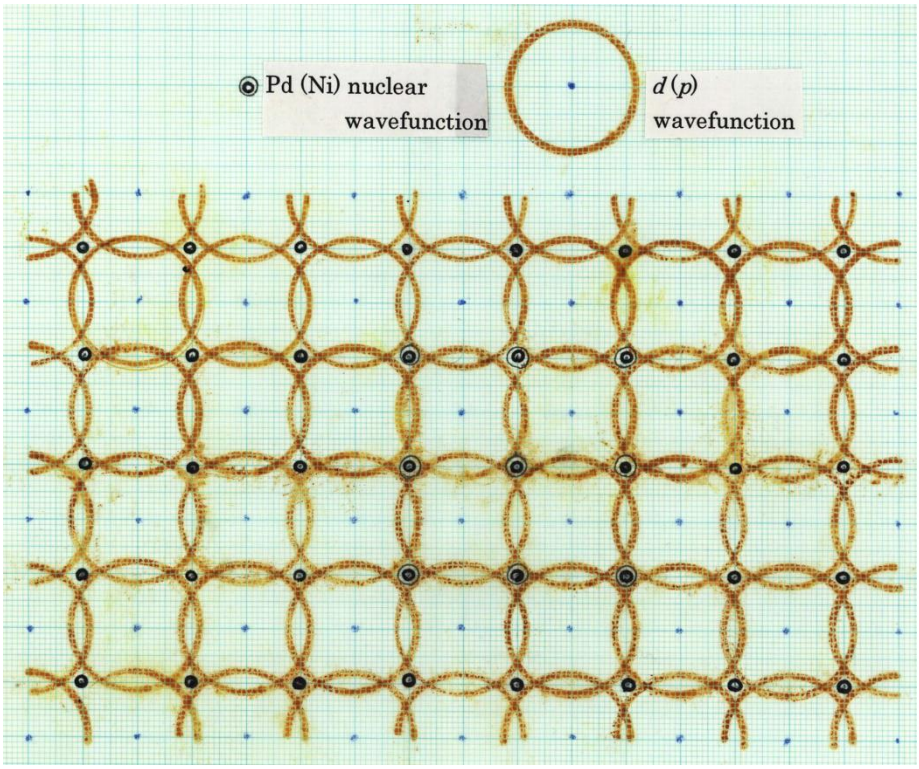

Fig. 5.4 Schematic two-dimensional figure of a superlattice PdD (NiH) formed of host atoms Pd (Ni) and deuterons (protons).

In Fig. 5.4, we have shown a schematic two-dimensional distribution of a superlattice PdD (NiH); The host atoms of Pd (Ni) distribute on lattice sites (in this case lattice sites of a square lattice) and deuterons (protons) distribute on each interstitial

sites. The wavefunction of a deuteron (proton) at an interstice in PdD (NiH) extends out to overlap with neutron wavefunctions of nuclei (small black points) on the nearest neighbor lattice sites (lattice nuclei) as shown schematically in the figure by a large circle.

If the neutrons in different lattice nuclei interact each other through the super-nuclear interaction shown in this Section 5.2.3, we can apply the idea of the electron energy band by tight binding summarized in Appendix A2 to the neutron energy band as discussed in Sec. 5.2.4.

5.2.1 Proton and Deuteron Wavefunctions at Interstices of CF Materials

There are two types of transition-metal hydrides/deuterides; one with localized hydrogen isotopes and another with non-localized ones. Therefore, the wavefunctions of a proton/deuteron at an interstice of the former have been able to depict as shown in Figs. 5.5 and 5.6. Figure 5.5 shows contour maps of the potential and the wavefunctions of an H atom in Ta in the case of TaH_x.

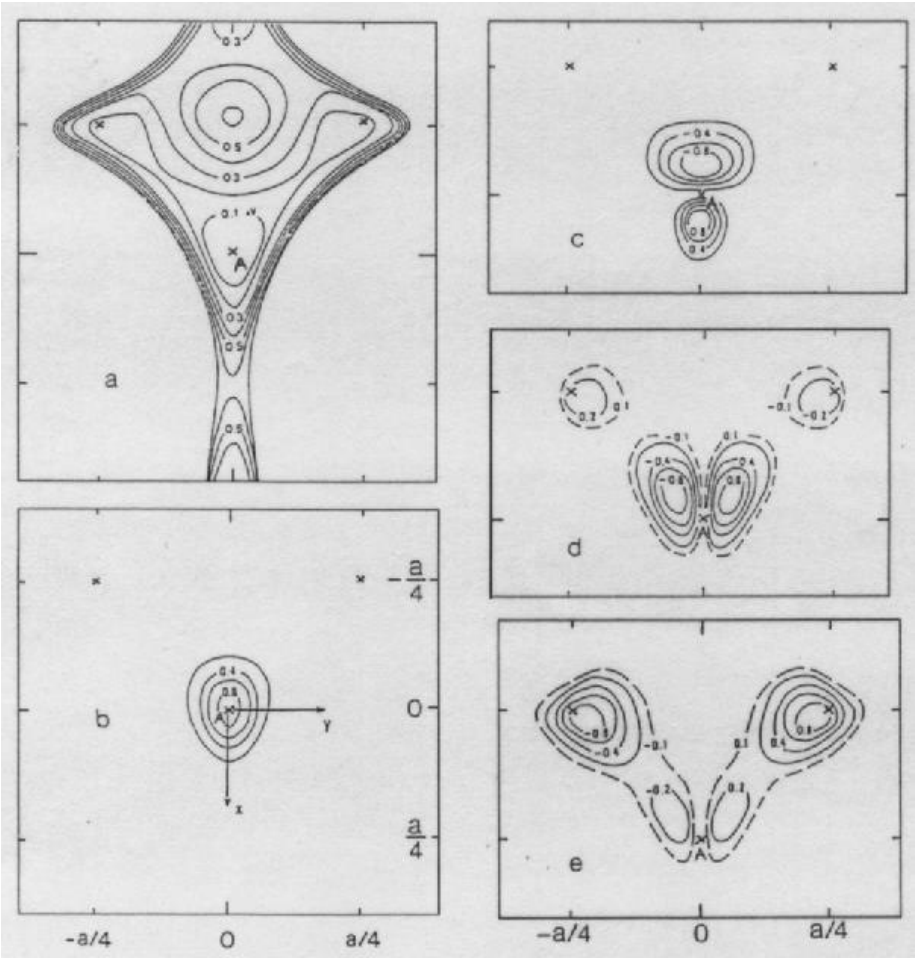

Fig. 5.5 Contour maps of the potential and the wavefunctions of an H atom in Ta. The H atom is self-trapped at the T site labeled A in the figures (*x*: the geometrical location of T sites on the *Z*-*X* plane.). (a) The potential; (b) the wavefunction of the ground state; (c) the first excited state, having a nodal plane at $Z = 0$; and (d) and (e) the excited states, both having a nodal plane at $X = 0$ [Fukai 2005 (Fig. 5.72)].

The maps in Fig. 5.5 depict the potential and the wave function on one of the cube faces of a bcc lattice, with the H atom localized on the T site labeled A in the figure.

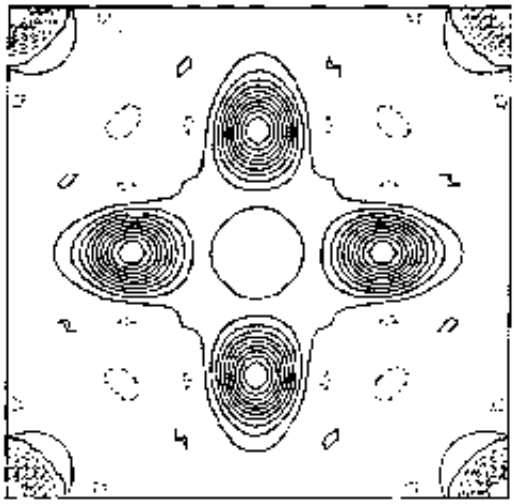

Fig. 5.6 Deuteron density contour maps in $VD_{0.79}$ at 70 ℃, Fourier-reconstructed from neutron diffraction data. [Fukai 2005 (Fig. 5.10)]

Figure 5.6 shows the deuteron density contour maps in $VD_{0.79}$ at 70 ℃ obtained by Fourier reconstruction of the neutron diffraction data.

As shown in Figs. 5.5 and 5.6, a proton or deuteron in bcc transition metals, which have been known as metals with low values of diffusion constants for hydrogen and deuterium, is localized at interstices even if they make transition between different interstices by hopping and tunneling.

In the case of the non-localized hydrides/deuterides, on the other hand, it is natural that we have not been able to depict the wavefunctions of a proton/deuteron in them. We can guess the non-localized, extended wavefunctions of protons/.deuterons in NiH_x and PdD_x ($x \approx 1$) from data of their physical properties such as diffusion constants and oscillation characteristics [Kozima 2004a, 2005, 2006].

5.2.2 Neutron States in Lattice Nuclei

The next component of the neutron band formation by the tight-binding mechanism is the neutron wavefunctions in nuclei at lattice sites. We have to take up two possible cases separately; (1) valence neutron states in ordinary stable nuclei and (2) neutron states in exotic nuclei.

5.2.2a Neutron States in Ordinary Nuclei at Ground State

The neutrons in ordinary nuclei in free space are stable and do not decay in contrast to a neutron in free space which decays by emission of an electron and a neutrino with a life time 889 ±3 s. The valence neutron orbital in a stable nucleus ${}^{A}_{Z}\mathrm{X}$ is successively occupied by a neutron when the atomic number A increases [Morfouace 2014] as cited in Sec. 4.2. Moving from ${}^{68}_{28}\mathrm{Ni}$ to ${}^{78}_{28}\mathrm{Ni}$ the neutron $1g_{9/2}$ orbital is filled. Similarly, moving from ${}^{102}_{46}\mathrm{Pd}$ to ${}^{110}_{46}\mathrm{Pd}$ the neutron $1g_{7/2}$ and $2d_{5/2}$ orbitals are filled.

Therefore, we can say in the case of a most popular CF material $\mathrm{NiH_x}$ (and $\mathrm{PdD_x}$), for example, that participation of neutrons to the neutron bands (*neutron bands of ground orbital*) is through the neutron valence states of nuclei ${}^{A}_{28}\mathrm{Ni}$ (${}^{A}_{46}\mathrm{Pd}$) at lattice sites in a super-lattice NiH (PdD) formed in a CF material $\mathrm{NiH_x}$ ($\mathrm{PdD_x}$). The valence neutron orbital of nuclei ${}^{A}_{28}\mathrm{Ni}$ (${}^{A}_{46}\mathrm{Pd}$) is $1g_{9/2}$ orbitals ($1g_{7/2}$ and $2d_{5/2}$ orbitals) in formation of neutron bands discussed in the following Sec. 5.2.3.

5.2.2b Neutron States in Ordinary Nuclei at Excited State

There is a possibility that neutron bands are formed by a combination of excited neutron orbitals at the evaporation level discussed in Sec. 4.1c. In this case, the neutron bands (*neutron bands of excited orbital*) are empty in the ground state of the system and are filled with neutrons supplied from outside or excited from lower levels in the lattice nuclei.

The excited neutron orbitals in ${}^{A}_{28}\mathrm{Ni}$ (${}^{A}_{46}\mathrm{Pd}$) are seen in Fig. 4.1 as $3s_{1/2}$ and $2d_{5/2}$ ($2f_{7/2}$ and $3p_{3/2}$). The orbitals of excited states are more extended in space and are favorable for the neutron band formation according to the tight-binding mechanism than the orbitals of ground states considered above.

Participation of the neutrons in the neutron bands of excited orbitals to the CFP may be temporal even if the effect is stronger than that of neutrons in the neutron bands made of ground orbital. The situation will be drastically changed if there is strong stabilization of the excited states by the interaction of neutrons and interstitial hydrogens. This effect will also be effective for the stabilization of neutron states in exotic nuclei discussed in the next section.

5.2.2c Neutron States in Exotic Nuclei

Exotic nuclei outlined in Sec. 4.2 are quasi-stable in their free state and decay spontaneously. It is, however, possible to assume that the exotic nuclei at lattice sites in interaction with hydrogen isotopes at interstitial sites (interstices) become stable due to the stabilization by the interaction with protons or deuterons. In such a case, we can use the extended neutron wavefunctions in the exotic nuclei at lattice sites for formation of the neutron bands (*neutron bands of exotic orbital*) by the tight-binding mechanism in place of the neutron wavefunction considered in the previous subsections. The rather large extension of the wavefunctions in the exotic nuclei works advantageously for the super-nuclear interaction mediated by interstitial hydrogen isotopes discussed in Sec. 5.2.3 and for formation of neutron bands by the tight-binding mechanism discussed in Sec. 5.2.4.

5.2.3 Super-nuclear Interaction between Neutrons in Different Lattice Nuclei in CF Material

In a superlattice composed of host atoms at lattice sites and protons or deuterons at interstices (e.g. NiH or PdD) in a CF material (e.g. NiH_x or PdD_x), shown schematically in Fig. 5.4, the neutrons in nuclei at different lattice sites have no such overlapping of their wavefunctions as in the case of electron wavefunctions shown in Figs. A4 (b) and A4 (c).

However, the wavefunctions of hydrogen isotopes in some transition metals are not localized at interstitial points (interstices) but extend out to cover the nearest neighbor lattice sites as experimental data on transition metal hydrides and deuterides show as shown in our previous paper [2014a (Appendices A3 and A4)].

In the case of such a superlattice as PdD or NiH as shown in Fig. 5.4, we can have a super-nuclear interaction between neutrons in different lattice nuclei in energy levels at the evaporation level (as shown in Fig. 4.1) mediated by deuterons or protons at interstices (as shown in Fig. 5.5) as shown before [Kozima 2004a, 2006].

To enforce our estimation of the super-nuclear interaction, we referred the neutron halo of neutron-rich exotic nuclei [Kozima 2006 (Sec. 3.5.3.1), 2014a (Appendix A2)]. It is true that the exotic nuclei have a finite life while the CFP is a result of long-term interaction of nucleons. Our excuse for this discrepancy rests on the possible new state induced by the stable existence of the CF-matter where the lattice nuclei and interstitial hydrogens interact through the nuclear force. Recognizing the limitations on our treatment of the CF materials, we proceed to explain the key concepts of the

super-nuclear interaction of lattice nuclei for the neutron bands and CF-matter.

The fundamental treatment of the calculation given before is cited here for convenience of explanation.

The overlapping of the proton wavefunction $\varphi_p(\boldsymbol{R}_j - \boldsymbol{b}_j)$ (or deuteron wavefunction $\varphi_d(\boldsymbol{R}_j - \boldsymbol{b}_j)$) on an interstice at $\boldsymbol{b}_j$ with a neutron wavefunction $\psi_n(\boldsymbol{x}, \boldsymbol{a}_i)$ on an adjacent lattice nucleus at $\boldsymbol{a}_i$ results in a proton-neutron interaction through the nuclear force (cf. Fig. 5.7). The nuclear interaction is expressed by a potential whose form is taken, for example, as the square-well type (neglecting spin-dependence and the imaginary part):

$$V_s(\boldsymbol{r} - \boldsymbol{R}) = -V^{(s)}_0, \qquad (|\boldsymbol{r} - \boldsymbol{R}| < b)$$
$$= 0, \qquad (|\boldsymbol{r} - \boldsymbol{R}| > b) \qquad (5.2.1)$$

where $V^{(s)}_0 \simeq 3.5$ MeV and $b \simeq 2.2\times10^{-13}$ cm for the neutron-proton interaction [Blatt 1952]. The choice of this potential out of several possible types does not make a large difference to the result for the low energy phenomena we are considering in this book.

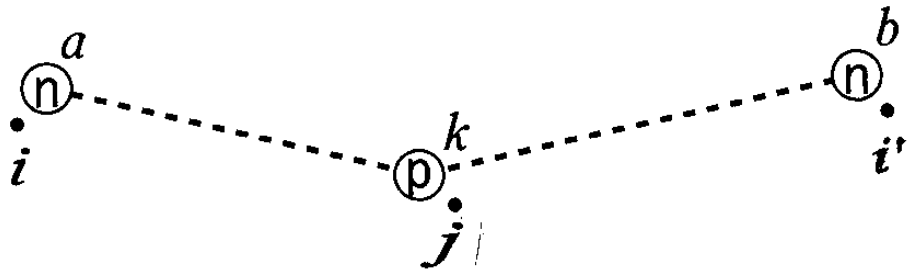

Fig. 5.7 Super-nuclear interaction between two neutrons ***a*** and ***b*** in lattice nuclei ***i*** and ***i'*** mediated by a proton *k* at an adjacent interstitial site ***j***.

It should be mentioned a word on the possible change of the potential (5.2.1) in the case of a neutron-deuteron interaction depicted in Fig. 5.8 from that in the case of a neutron-proton interaction described above. It is possible to have somewhat different values of $V^{(s)}_0$ and b for the neutron-deuteron interaction from those given above for the neutron-proton interaction. This possible difference will influence the neutron band formation in protium and in deuterium CF materials which may result in the different CFP in these systems observed clearly by experiments.

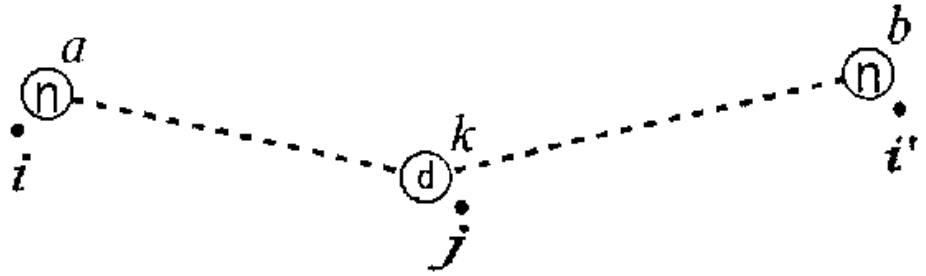

Fig. 5.8 Super-nuclear interaction between two neutrons ***a*** and ***b*** in lattice nuclei ***i*** and ***i'*** mediated by a deuteron *k* at an adjacent interstitial site ***j***.

The interaction between a neutron in a lattice nucleus and an interstitial proton (or deuteron) pulls two neutron states in different lattice nuclei into coupling as shown below. We will call this coupling the "super-nuclear interaction" [Kozima 2006 (Sec. 3.7.2)]. In the following investigation, we concentrate on excited neutrons rather than on protons in lattice nuclei, which need more energy to be raised to the excited levels due to the fact $Z << N$. (In Pd, Z = 46 and N = 56－64.). Further, the neutron-proton interaction might be more long-range than proton-proton interaction as we noticed in elsewhere [Kozima 2006 (Subsection 3.5.3)].

If there is an interaction between a neutron in a lattice nucleus and a proton/deuteron at an interstice $\boldsymbol{b}_\mathrm{j}$ next to the lattice site $\boldsymbol{a}_\mathrm{i}$ where the lattice nucleus is, there appears an interaction between two neutrons in two different lattice nuclei at $\boldsymbol{a}_\mathrm{i}$ and $\boldsymbol{a}_{\mathrm{i}'}$ interacting with the same proton/deuteron when $\boldsymbol{a}_{\mathrm{i}'}$ is also a neighbor of $\boldsymbol{b}_\mathrm{j}$ as shown in Figs. 5.7 and 5.8 for a proton and a deuteron, respectively. The coupled neutrons in lattice nuclei reveal a dispersed energy spectrum called the energy band by the tight-binding as already explained using the electron energy band in Appendix A2. We investigate this possibility rather qualitatively in this Subsection.

(a) Total Energy of *fcc* Transition-Metal Hydrides and Deuterides

In the second-order perturbation approximation taking the square well potential (5.2.1) for the nuclear interaction, the total energy $E_{\mathrm{k},\{\mathrm{p}\alpha\}}$ of this system composed of occluded protons (deuterons) and neutrons in an excited level of lattice nuclei expressed as a Bloch state is written down as follows [Kozima 2004a, 2006 (Sec. 3.7.2.1)]:

$$E_{\mathrm{k},\{\mathrm{p}\alpha\}} = E_{\{\mathrm{n},\,\mathrm{p}\alpha\}} + \sum_{\mathrm{k}',\,\mathrm{i},\,\mathrm{i}',\,\mathrm{j}} \exp[-\mathrm{i}(\boldsymbol{k}\boldsymbol{a}_\mathrm{i} - \boldsymbol{k}'\boldsymbol{a}_{\mathrm{i}'})]\; v_\mathrm{np}(ii'j) \tag{5.2.2}$$

$$E_{\{\mathrm{n},\,\mathrm{p}\alpha\}} = E_{\{\mathrm{n}\}}{}^{(\mathrm{p})} + \sum_\mathrm{j}\varepsilon_\mathrm{pj}, \tag{5.2.3}$$

$$v_\mathrm{np}(ii'j) = \sum_{\{\mathrm{p}'\}\neq\{\mathrm{p}\}} \mathrm{P}\int \mathrm{d}E\; \rho_\mathrm{n}(E)\; (\langle np;ij|V|n'p';ij\rangle(\langle n'p';i'j|V|np;i'j\rangle)/(E+\varepsilon_{\mathrm{p}'\mathrm{p}}), \tag{5.2.4}$$

$$V(\boldsymbol{r}) = V_\mathrm{s}(\boldsymbol{r}), \tag{5.2.5}$$

$$\langle np;ij|V|n'p';ij\rangle = \iint \mathrm{d}\boldsymbol{r}\mathrm{d}\boldsymbol{R}_\mathrm{j}\; \psi_{\{\mathrm{n}\}}{}^*(\boldsymbol{r}-\boldsymbol{a}_\mathrm{i})\varphi_\mathrm{p}{}^*(\boldsymbol{R}_\boldsymbol{j}-\boldsymbol{b}_\mathrm{j})\; V_\mathrm{s}(\boldsymbol{r}-\boldsymbol{R}_\mathrm{j})\psi_{\{\mathrm{n}'\}}{}^*(\boldsymbol{r}-\boldsymbol{a}_\mathrm{i})\;\varphi_{p'}{}^*(\boldsymbol{R}_\boldsymbol{j}-\boldsymbol{b}_\mathrm{j}), \tag{5.2.6}$$

where summations over *i* and *i*' in Eq. (5.2.2) are only over the nearest neighbor lattice sites $\boldsymbol{a}_\mathrm{i}$ and $\boldsymbol{a}_{\mathrm{i}'}$ of an interstice $\boldsymbol{b}_\mathrm{j}$, $\rho_\mathrm{n}(E)$ is a density of states for neutron quantum states, and

$\varepsilon_{\mathrm{p}'\mathrm{p}} \equiv \varepsilon_{\mathrm{p}'} - \varepsilon_\mathrm{p}$, $E \equiv E_{\{\mathrm{n}'\}} - E_{\{\mathrm{n}\}}$.

Further, the summation over *p*' in (5.2.4) reduces to $(n_\mathrm{p}+1)(n_\mathrm{p}+2)$, the degeneracy of

the energy ε_{np}, times summation over n_p. $E_{\{n\}}{}^{(p)}$ is an energy of a neutron in an excited state $\psi_{\{n\}}(\boldsymbol{r} - \boldsymbol{a}_i)$ in a lattice nucleus at $\boldsymbol{a}_i$ when occluded protons are in states p_α, and ε_{pj} in Eq. (5.2.3) is an energy of a proton in a state $\varphi_{pj}(\boldsymbol{R_j} - \boldsymbol{b}_j)$ at an interstice $\boldsymbol{b}_j$. We ignore, however, *p*-dependence of $E_{\{n\}}{}^{(p)}$ hereafter in this work.

Thus, the matrix elements (5.2.6) calculated for neutron states around the separation level and proton (deuteron) states of Bloch functions are at most 10^{20} times larger than the value calculated for a lower excited state of a neutron in nucleus and a localized state of a proton (deuteron). If this matrix element is effective, there appears an interaction (5.2.4) between two neutrons in different lattice nuclei mediated by occluded hydrogen isotopes at interstitials. This interaction is a long-range one reaching from a lattice site to another having its origin in the internucleon strong interaction (5.2.1); we may call it the *super-nuclear interaction* between neutrons in different lattice nuclei in transition-metal hydrides and deuterides. The super-nuclear interactions are illustratively depicted in Fig. 5.7 for NiH and in Fig. 5.8 for PdD.

Finally, the effective potential $v_{np}(ii'j)$ (5.2.4) is calculated as a function of the principal value of the integration which appeared in that equation using the result of an order of magnitude calculation [Kozima 2004a]

$$<np;ij|V|n'p';ij> = 3.2\times10^{-14}, \quad \text{(eV)} \tag{5.2.7}$$

and assuming the insensitiveness of the matrix elements to the energy:

$$v_{np}(ii'j) = 1\times10^{-27}\, I\ (\text{eV})^2, \tag{5.2.8}$$

$$I \equiv \mathrm{P}\int \mathrm{d}E\ \rho_n(E)/E.$$

We can, then, estimate the approximate value of the integral (principal value) *I*, taking following values $\rho_n(E) \simeq 10^3\ \text{keV}^{-1}$, $\delta\varepsilon \simeq 10^{-3}$ keV, and $\triangle\varepsilon \simeq 1$ keV on the assumption that single-particle energy-level difference is $\simeq 1$ keV and the level density increases to 10^3 times larger than that of single particle motion:

$$I \simeq \rho_n(\varepsilon)\triangle\varepsilon/\delta\varepsilon = 10^6 \quad \text{eV}^{-1}. \tag{5.2.9}$$

Thus, an order of magnitude of $v_{np}(ii'j)$ in PdH becomes

$$v_{np}(ii'j) \simeq 1\times10^{-24}\ (\text{eV}). \tag{5.2.10}$$

Including the enhancement factors defined to take several effects [Kozima 2004a], we obtain the final result:

$$v_{np}(ii'j) \simeq 1\times10^{-24}\ \alpha^2\beta^2 \quad \text{(eV)}. \tag{5.2.11}$$

where $\alpha_{max}{}^2 = 10^{12}$ and $\beta_{max}{}^2 = 10^{20}$.

5.2.4 The Tight-binding Neutron Bands

To show briefly the crystal-structure dependence of the bandwidth Δ of the neutron valence band, we will make a simplification of the super-nuclear interaction (5.2.6)

between adjacent nuclei at a_i and $a_{i'}$ assuming that it depends only on the magnitude of the vector $a_l \equiv a_i - a_{i'}$.

Then, we can rewrite the total energy (5.2.2) and have the energy spectrum of the neutron Bloch waves in the *fcc* lattice (a is the side of the lattice cube);

$$\varepsilon_k = E_{\{n,p\}} - \gamma_{n,p} - 2\times 4\gamma'_{n,p}(\cos k_y a/4 \cos k_z a/4 + \cos k_z a/4 \cos k_x a/4 + \cos k_x a/4 \times \cos k_y a/4) - 2\gamma'_{n,p}(\cos k_x a + \cos k_y a + \cos k_z a), \quad (5.2.12)$$

$$E_{\{n,p\}} = E_{\{n\}} + \sum_j \varepsilon_{pj}, \quad (5.2.13)$$

$$-\gamma_{n,p} = v_{np}(0), \quad (5.2.14)$$

$$-\gamma'_{n,p} = v_{np}(ii'j). \quad (5.2.15)$$

The shifts $\gamma_{n,p}$ of energy level $E_{\{n,p\}}$ may be negative in appropriate situations. A characteristic of this energy band formation is the contributions not only from nearest neighbors ((0, $\pm a/2$, $\pm a/2$), etc.) but also from next nearest neighbors (($\pm a$, 0, 0), etc.)

Putting the value $v_{np}(ii'j) \simeq 1 \times 10^{-24}\, \alpha^2\beta^2$ in Eq. (5.2.15), we obtain the bandwidth Δ from (5.2.12) as follows:

$$\Delta \simeq 2.5\times 10^{-23}\alpha^2\beta^2 \quad \text{(eV)}. \quad (5.2.16)$$

The value of the bandwidth $\Delta \simeq 2.5$ GeV for $\alpha_{max} = 10^6$ and $\beta_{max} = 10^{10}$ is obtained by the assumptions that the level density at excited levels around the evaporation energy is similarly strongly magnified by collective modes as observed by neutron resonance absorption experiments and that the excited proton states are expressed by plane waves. The first assumption has no experimental basis at present and seems too exaggerated the situation to be real. We may assume rather small value as $\alpha = 10^2$ or 10^3 instead of 10^6. Then, the bandwidth may have a value about $\Delta \simeq 1 - 10^2$ eV for $\beta = \beta_{max}$.

The assumption, on the other hand, of a plane wave for the proton (deuteron) Bloch state ($\beta_n = 10^{10}$) may overestimate the matrix elements (5.2.8) by several orders of magnitude making the bandwidth down to $\Delta \simeq 10^{-2} - 1$ eV if we take $\beta = 10^8 - 10^9$.

On the other hand, if the bandwidth Δ is less than the thermal energy $\simeq 25$ meV of ions at room temperature, the concept of the neutron band may be not realistic and the neutrons should be treated as localized at lattice nuclei. This requires $\alpha^2\beta^2 > 10^{21}$ for a realistic neutron valence band. This means that the parameters to realize the neutron valence band should be $\alpha > 10^{5.5}$ for $\beta = 10^5$ and $\beta > 10^7$ for $\alpha = 10^3$. [Kozima 2006 (Secs. 3.5 – 3.7), 2008, 2011]

We have developed the neutron bands by the tight-binding approximation using the neutron wavefunctions at around the evaporation level. In the calculation we assumed the wavefunctions be rather extended out over the nuclear boundary of usual nuclei assuming they are the neutrons in exotic nuclei with excess neutron numbers N over the proton numbers Z investigated extensively in recent years (e.g. [Cizewski 2010, Utsuno

2014]).

This assumption may be tolerable if we consider the favorable situation for the exotic nuclei at lattice sites in CF materials which interacts each other through the super-nuclear interaction mediated by protons/deuterons at interstices thus lowing their energy to stabilize the state which is not necessarily stable in an isolated nucleus.

Therefore, in the situation where host nuclei occupy a sublattice (host sublattice) and protons/deuterons another sublattice (proton/deuteron sublattice) forming a superlattice, we have to accept a feature of solid-state nuclear physics not explored before which has been announced by the mysterious phenomenon, the CFP as we have called it, including effects only explained by occurrence of nuclear reactions in solids at around room temperature without any acceleration mechanisms.

5.2.5 Stability of neutrons in the tight-binding neutron band

Neutrons with wavefunctions used in the tight-binding approximation for the neutron bands are in stable states in the lattice nuclei. As recent treatments of single-particle structure of exotic nuclei with large excess of neutrons show, we can use the wavefunction of a neutron in an nucleon orbit independently of remaining nucleons in a nucleus (e.g. [Cizewski 2010, Utsuno 2014]). This is the way we calculated the neutron bands using the tight-binding approximation in Sec. 5.2.4 and in the previous books and papers [Kozima 2004a, 2005, 2006, 2014a].

Thus, the band neutrons made of stable neutron states in lattice nuclei have stability inherent to the original states. This is the reason that the neutrons in the bands made of neutron wavefunctions in lattice nuclei are stable against the beta-decay in contrast to the neutrons in the bands made of wavefunctions of free neutrons.

6. Discussions and Conclusion

The development of experimental investigation on the CFP in this quarter of a century since 1989 have substantiated existence of nuclear reactions in CF materials (e.g. PdD_x, NiH_x, and so forth) at near room temperature without any acceleration mechanisms. This fact has been partially confirmed by scientists outside this field in many documents and papers including the DOE Report published in 2004 [DOE 2004].

Despite of the increasing reality of the CFP, there has not been achieved establishment of its science yet. We have tried to give a self-consistent explanation of wide-spread various experimental facts obtained in this field using a phenomenological approach. Fortunately enough, it may be possible to say that our approach has been fairly successful to give qualitative and sometimes semi-quantitative explanations for

experimental values of observables and for numerical relations between observables.

In application of our model, we used a key premise, existence of the "trapped neutrons" with a density n_n, an adjustable parameter, in CF materials [Kozima 1994, 1998a, 2004a, 2006, 2014a]. The justification of the premise based on the quantum mechanical investigation has been tried in several papers [Kozima 2004a, 2006, 2009a]. The trial is in its infantile stage at present even if a hint to justify the premise was depicted [Kozima 2004a, 2006 (Sec. 3.7)].

In the Preface to his book, R. Golub cited a word by Maier-Leibnits as follows;
"*Maier-Leibnitz once said that he was always surprised to see how a simple little idea could grow and grow until it resulted in something large and complex with implications for other fields of research.*" [Golub 1990 (Preface)]

We hope that the idea of the "trapped neutron" in CF materials becomes "the simple little idea" Maier-Leibnits told.

Therefore, in the situation where host nuclei occupy a sublattice (host sublattice) and protons/deuterons another sublattice (proton/deuteron sublattice) forming a superlattice, we have to accept a new feature of solid-state nuclear physics not explored before but announced by the mysterious phenomenon, we have called the cold fusion phenomenon CFP), including effects only explained by occurrence of nuclear reactions in solids at around room temperature without any acceleration mechanisms.

The TNCF model proposed by us in 1993 and developed since then has given a unified explanation of experimental data in the CFP [Kozima 1998a, 2006, 2014a, 2014b, 2014c]. To explain the premises of the model quantum mechanically, we have used novel knowledge obtained in nuclear physics and in solid state physics and proposed an idea of the neutron band where neutrons are trapped and are participating in the nuclear reactions for the CFP. The neutron bands in CF materials NiH_x and PdD_x are explained in our books [Kozima 2004a, 2006], papers [Kozima 2005, 2009a] and in this paper (Sec. 5).

There are possible differences in the characteristics of neutron bands in NiH and in PdD depending on the neutron orbitals composing the neutron bands. As discussed in Sec. 5.2.2a, the neutrons in ${}^{A}_{28}$Ni are in $1g_{9/2}$ orbital while those in ${}^{A}_{46}$Pd are in $1g_{7/2}$ and $2d_{5/2}$ orbitals. The difference of these orbitals in addition to the wavefunctions of hydrogen isotopes at interstices may influence the characteristics of the neutron bands.

The angular dependences of wavefunctions in spherically symmetric H.O. potentials are shown in Fig. 6.1 for the nucleon densities in the x-z plane.

$$E_{nl} = \hbar\omega\left(2n + l + \frac{3}{2}\right)$$

(n, l, m)

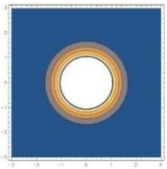

$\frac{3}{2}\hbar\omega$

(0,s,0)

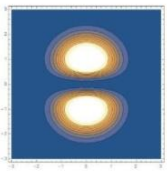

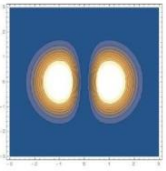

$\frac{5}{2}\hbar\omega$

(0,p,0) (0,p,1)

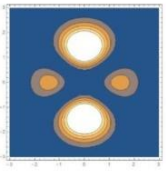

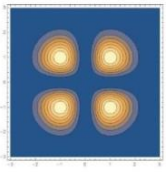

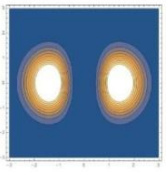

$\frac{7}{2}\hbar\omega$

(1,s,0) (0,d,0) (0,d,1) (0,d,2)

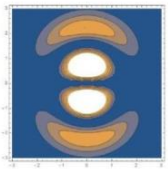

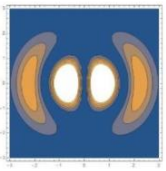

(1,p,0) (1,p,1)

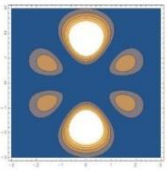

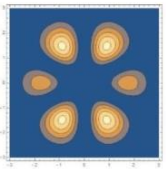

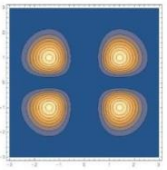

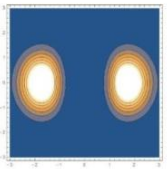

$\frac{9}{2}\hbar\omega$

(0,f,0) (0,f,1) (0,f,2) (0,f,3)

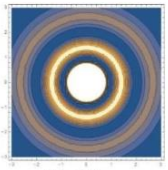

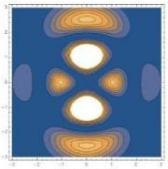

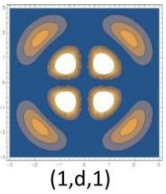

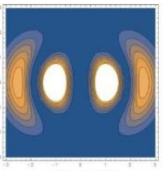

(2,s,0) (1,d,0) (1,d,1) (1,d,2)

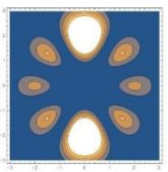

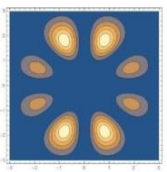

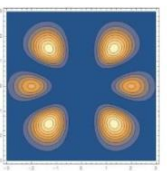

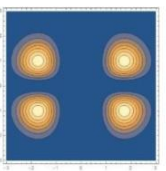

(0,g,0) (0,g,1) (0,g,2) (0,g,3)

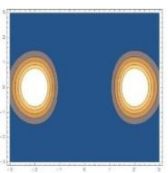

$\frac{11}{2}\hbar\omega$

(0,g,4)

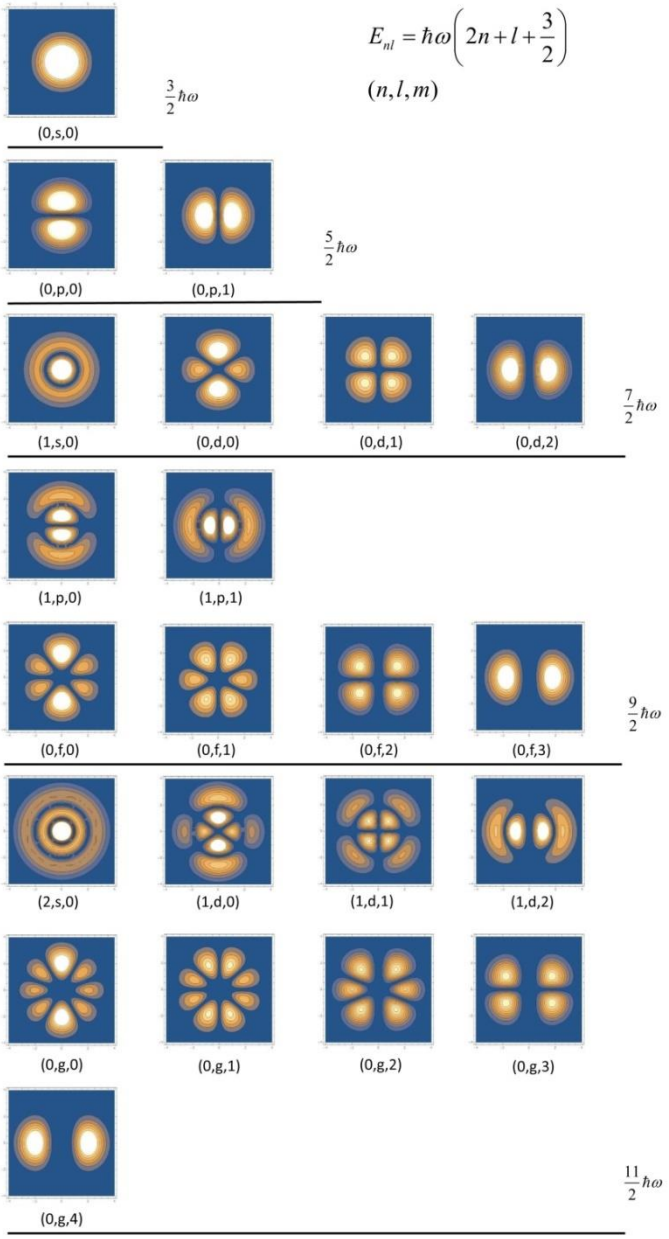

Fig. 6.1 Nucleon densities of the states with quantum numbers (*n. l. m*) in a spherical H.O. potential in the x-z plane.

The valence neutron band in NiH is made only of $1g_{9/2}$ orbital while that in PdD is of $1g_{7/2}$ and $2d_{5/2}$ orbitals. This difference in the symmetry of the composite orbitals as illustrated in Fig. 6.1 may influence the characteristics of the cf-matter in NiH and in PdD.

Furthermore, the difference of the interaction potential $V_{\text{n-p}}$ and $V_{\text{n-d}}$ written down in

Eqs. (6.1) and (6.2) may influence the band structures in NiH and PdD where b's are the effective scattering lengths, while we have no definite values of these b's at present as discussed below.

$$V_{n\text{-}p}(r) = (2\hbar^2 b_{n\text{-}p}/m)\delta(r)/r^2, \quad (6.1)$$

and

$$V_{n\text{-}d}(r) = (2\hbar^2 b_{n\text{-}d}/m)\delta(r)/r^2. \quad (6.2)$$

Therefore, difference in the characteristics of the CFP observed in NiH_x and PdD_x [Kozima 1998a (Tables 11.2 and 11.3), 2006 (Tables 2.2 and 2.3)] might be deduced from the difference in the symmetry of the neutron bands in these CF materials described in Sec. 5.2.4.

It should be mentioned about the interaction potential between a neutron and a deuteron corresponding to Eq. (5.2.1) for the neutron-proton interaction. There is surely a difference in the neutron-proton interaction $V_{n\text{-}p}$ and the neutron-deuteron interaction $V_{n\text{-}d}$ which induce the difference in the CFP in protium and in deuterium CF materials. We have, however, no definite form of the interaction potential for the neutron-deuteron interaction applicable to the super-nuclear interaction (5.2.4) we are considering in relation to the CFP. It is clear that the potentials (6.1) and (6.2) differs each other as the interactions observed by scattering and absorption experiments show big differences as shown in Figs. 6.2 and 6.3.

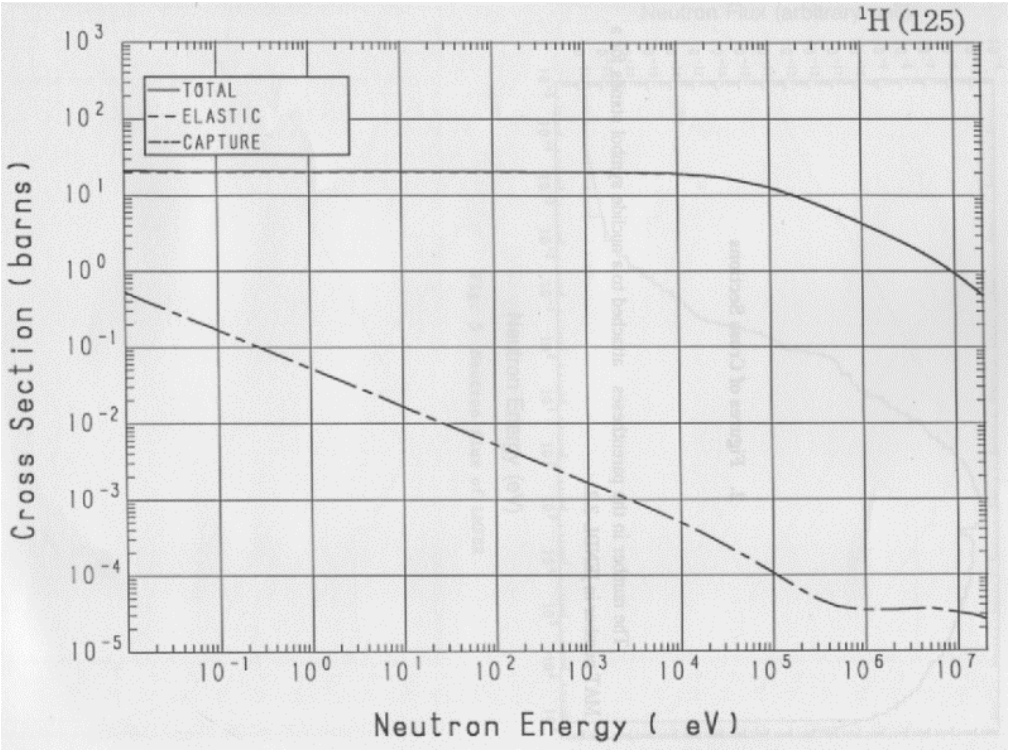

Fig. 6.2 Neutron scattering and absorption cross-sections by proton $^1_1$H [JAERI 1997].

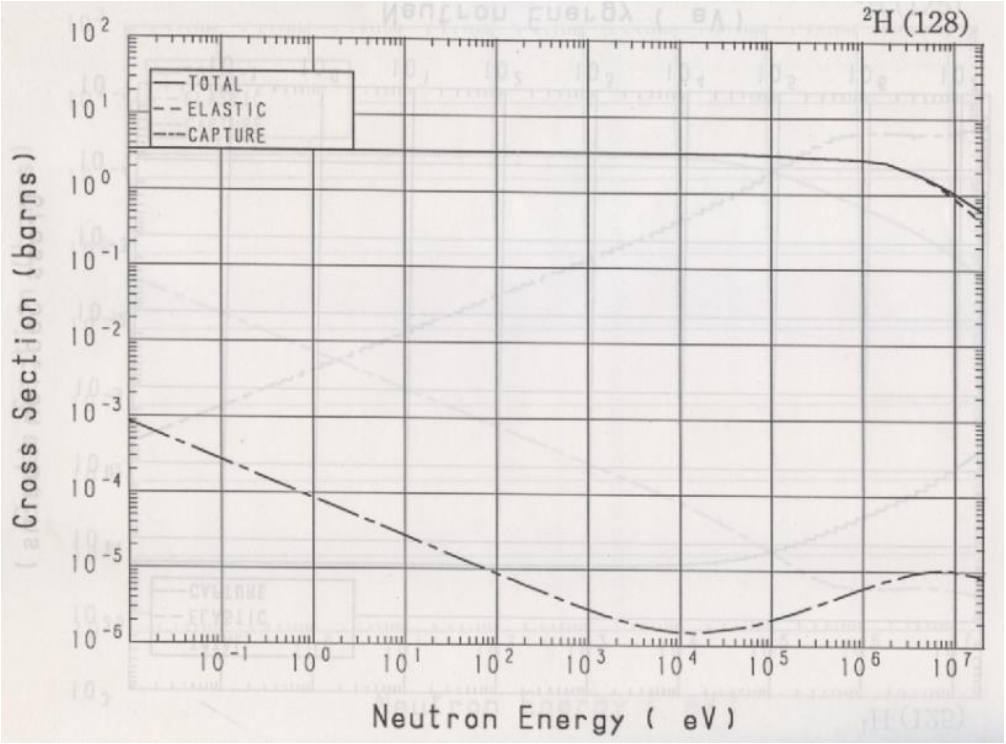

Fig. 6.3 Neutron scattering and absorption cross-sections by deuteron $^{2}_{1}$H [JAERI 1997].

Even if our approach to the CFP is in its infantile stage, we can deduce some conclusions on nuclear physics and on solid state physics from the investigation of the CFP using the phenomenological model.

One is the reward to nuclear physics from the CFP. The neutron bands introduced for the explanation of events in the CFP give new insight into the neutron-lattice nuclei interaction. It might be possible to have a stable exotic nuclei interacting with protons or deuterons at interstices in CF materials.

Another is the reward to solid state physics from the CFP. If the neutron bands are real and effective for the CFP as we contemplated in our discussion [Kozima 2006, 2014a], the interstitial protons or deuterons in CF materials are stabilized by the super-nuclear interaction and have larger diffusibility as observed in experiments in PdH_x , PdD_x, NiH_x, and NiD_x. It is possible to imagine that the low-energy state of protons/deuterons is similar to Cooper pair state in the superconductivity of electrons with an energy gap for electron excitation up to higher energy states.

The physics of transition-metal hydride/deuteride is essentially the physics of

superlattices made of the host metal and the proton/deuteron sublattices, from our point of view. The phenomena accompanied to the neutron band formation are the cold fusion phenomenon on the nuclear phase and the high diffusibility of protons/deuterons on the atomic phase. The CFP observed in CF materials is the physics of neutrons in such superlattices as NiH, PdD and C_xH and is a new field not noticed before at all. The CFP promises vast new development of science and technology based on this new state formed by lattice nuclei and interstitial hydrogen isotopes.

Appendix

The electron energy band is reviewed as a model of the neutron energy band proposed in our treatment of the trapped neutron catalyzed fusion model. The two contrastive approaches to the band, one from the free state another from bound state, are applicable also to the case of the neutrons in solids as used in Section 4.

A1 Quasi-Free Electron Approximation

The quasi-free (or nearly free) electron approximation to the energy band of electrons in solids uses a perturbation approach to the electrons in solids; the effect of crystalline array of atoms on the free electron is introduced into calculation as a perturbation on the free electron state.

The free electron wavefunctions are of the form

$$\psi_{\boldsymbol{k}}(\boldsymbol{r}) = \exp(i\boldsymbol{k}\cdot\boldsymbol{r}) \qquad \text{(A.1)}$$

they represent running waves and carry momentum $p = \hbar k$. (e.g. [Kittel 1976 (Chapter 7)]).

We know that Bragg reflection is a characteristic feature of wave propagation in crystals where a free electron feels such a potential energy described in Fig. A1 (a) in a linear lattice.

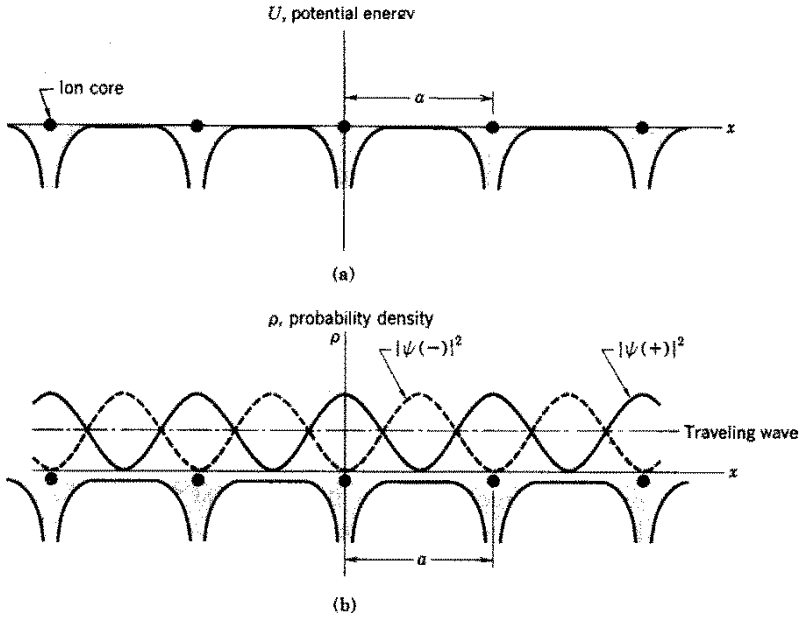

Fig. A1 (a) Variation of potential energy of a conduction electron in the field of the ion cores of a linear lattice. (b) Distribution of probability density in the lattice for $|\psi(-)|^2 = \sin^2 \pi x/a$; $|\psi(+)|^2 = \cos^2 \pi x/a$; and for a traveling wave. The wavefunction $\psi(+)$ piles up electronic charge on the cores of the positive ions, thereby lowering the potential energy in comparison with the average potential energy seen by a traveling wave. The wave function $\psi(-)$ piles up charge in the region between the ions and removes it from the ion cores; thereby raising the potential energy in comparison with that seen by a traveling wave. This figure is the key to understanding the origin of the energy gap. [Kittel 1976 (Fig. 7.3)]

The Bragg condition $(k + G)^2 = k^2$ for diffraction of a wave of wavevector k becomes in one dimension

$$k = \pm(1/2)G = \pm n\pi/a. \qquad \text{(A.2)}$$

where $G = 2\pi n/a$ is a reciprocal lattice vector and n is an integer.

At $k = \pm\pi/a$ the wavefunctions are not the traveling waves $\exp(i\pi x/a)$ and $\exp(-i\pi x/a)$ of the free electron model. We can form two different standing waves from the traveling waves $\exp(i\pi x/a)$ and $\exp(-i\pi x/a)$ as shown in Fig. A1 (b):

$$\psi(+) = \exp(i\pi x/a) + \exp(-i\pi x/a) = 2\cos(\pi x/a) ;$$
$$\psi(-) = \exp(i\pi x/a) - \exp(-i\pi x/a) = 2\sin(\pi x/a). \qquad \text{(A.3)}$$

The wavefunctions at the zone boundary are

$\sqrt{2}\cos\pi x/a$ and $\sqrt{2}\sin\pi x/a$

normalized over unit length. We write the crystal potential as

$U(x) = U \cos 2\pi x/a$ (A.4)

Then, the energy difference in first order between the two states is

$E_g = 2U\int dx\, (\cos 2\pi x/a)\, (\cos^2 \pi x/a - \sin^2 \pi x/a) = U$. (A.5)

The gap is equal to the amplitude of the Fourier component of the crystal potential $U(x)$. [Kittel 1976]

Thus, we understand the origin of the gap in the energy spectrum of electrons in solids using this model. Often the band structure can be explained on this model; we shall also find some situations where it is not applicable.

It is useful to investigate the same problem with another simple potential depicted in Fig. A2 instead of the one described by Eq. (A.4).

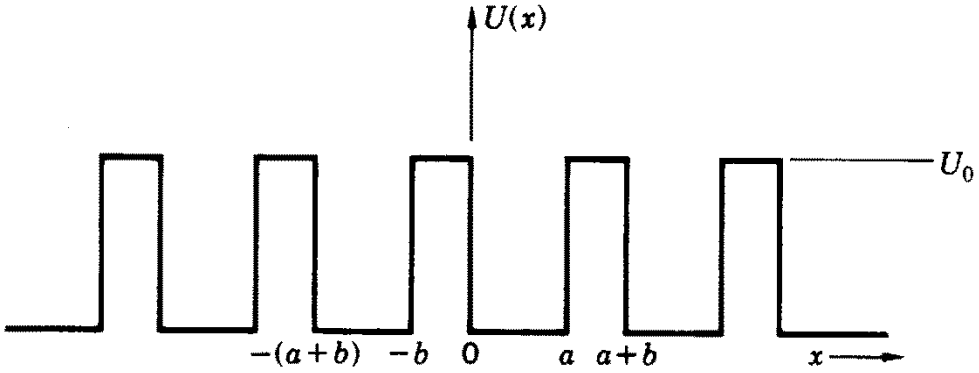

Fig. A2 Kronig-Penny potential $U(x)$ vs. x (after [Kittel 1976 (Fig. 7.4)])

In the Kronig-Penny potential shown in Fig. A2, the energy spectrum of an electron forms a band structure depicted in Fig. A3 instead of the continuous spectrum of a free electron depicted also there by a dotted line.

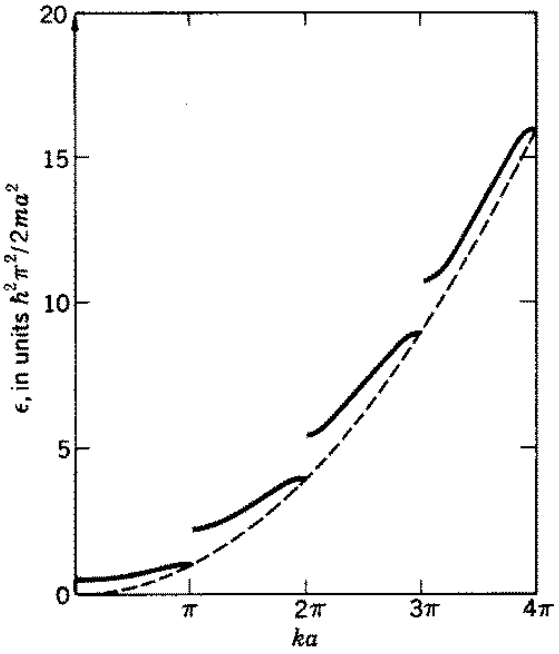

Fig. A3 Band structure ε vs. ka of Kronig-Penny potential where ε is the energy of electron, k is the wave number and a is the width of potential well as depicted in Fig. A2 (after [Kittel 1976 (Fig. 7.6)]).

The OPW (orthogonalized plane wave) method, a generalized quasi-free electron approximation, has been widely applied to alkaline metals successfully to explain their electronic properties. [Callaway 1958, Kozima 1961].

A2 Tight-Binding Electron Approximation

The energy band of electrons in crystals keeping the original characteristics of energy levels of atoms composing the crystal is investigated using the so-called tight-binding approximation.

Let us consider a situation where two hydrogen atoms brought together to overlap their electron wavefunctions as shown in Fig. A4.

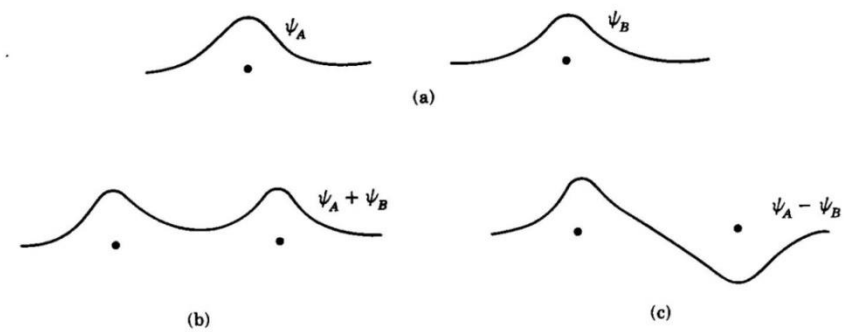

Fig. A4 (a) Schematic drawing of wavefunctions of electrons on two hydrogen atoms at large separation. (b) Ground state wavefunction at closer separation. (c) Excited state wavefunction [Kittel 1976 (Fig. 9-16)].

As free atoms are brought together, the coulomb interaction between the atom cores and the electron splits the energy levels, spreading them into bands as shown schematically in Fig. A5. Each state of given quantum number of the free atom is spread in the crystal into a band of energies. The width of the band is proportional to the strength of the overlap interaction between neighboring atoms.

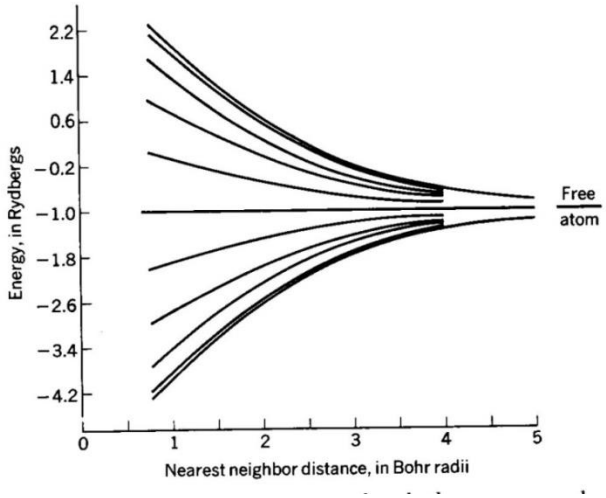

Fig. A5 The 1s band of a ring of 20 hydrogen atoms; the one-electron energy calculated in the tight-binding approximation with the nearest-neighbor overlap integral of Eq. (3.9) [Kittel 1976 (Fig. 9.17)].

Suppose that the ground state of an electron moving in the potential $U(r)$ of an isolated atom is $\varphi(\mathrm{r})$ and that the energy is E_0; suppose φ is an s state, for simplicity. If the influence of one atom on another is small, we obtain an approximate wavefunction for one electron in the whole crystal by taking

$$\psi_{\mathbf{k}}(\boldsymbol{r}) = \sum_{\mathrm{j}} C_{\boldsymbol{k}\mathrm{j}}\varphi(\boldsymbol{r} - \boldsymbol{r}_{\mathrm{j}}) \qquad \text{(A.6)}$$

where the sum is over all lattice sites. We assume the primitive basis contains one atom. This function is of the Bloch form if $C_{\boldsymbol{k}j} = N^{-1/2}\exp(\mathrm{i}\boldsymbol{k}\cdot\boldsymbol{r}_{\mathrm{j}})$, which gives, for a crystal of N atoms,

$$\psi_{\mathbf{k}}(\boldsymbol{r}) = N^{-1/2}\sum_{\mathrm{j}}\exp(\mathrm{i}\boldsymbol{k}\cdot\boldsymbol{r}_{\mathrm{j}})\varphi(\boldsymbol{r} - \boldsymbol{r}_{\mathrm{j}}). \qquad \text{(A.7)}$$

We find the first-order energy by calculating the diagonal matrix elements of the Hamiltonian of the crystal:

$$\langle \mathrm{k}|\mathrm{H}|\mathrm{k}\rangle = N^{-1}\sum_j\sum_m \exp[i\boldsymbol{k}\cdot(\boldsymbol{r}_j - \boldsymbol{r}_{\boldsymbol{m}})]\ \langle\varphi_{\mathrm{m}}|\mathrm{H}|\varphi_{\mathrm{j}}\rangle, \qquad \text{(A.8)}$$

Where φ_m $=\boldsymbol{\varphi(r - r_m)}$. Writing $\boldsymbol{\rho}_m = \boldsymbol{r}_m - \boldsymbol{r}_j$,

$$<k|H|k> = \sum_m \exp(i\boldsymbol{k}\cdot\boldsymbol{\rho}_m) \int dV \varphi^*(\boldsymbol{r} - \boldsymbol{\rho}_m) H\varphi(\boldsymbol{r}) \quad \text{(A.9)}$$

We now neglect all integrals in (A.9) except those on the same atom and those between nearest neighbors connected by $\boldsymbol{\rho}$. We write

$$\int dV \varphi^*(\boldsymbol{r}) H\varphi(\boldsymbol{r}) = -\alpha, \quad \int dV \varphi^*(\boldsymbol{r} - \boldsymbol{\rho}) H\varphi(\boldsymbol{r}) = -\gamma; \quad \text{(A.10)}$$

and we have the first-order energy, provided $<k|k> = 1$:

$$<k|H|k> = -\alpha - \gamma \sum_m exp(i\boldsymbol{k}\cdot\boldsymbol{\rho}_m) = \varepsilon_{\boldsymbol{k}}. \quad \text{(A.11)}$$

The dependence of the overlap energy γ on the interatomic separation $\boldsymbol{\rho}$ can be evaluated explicitly for two hydrogen atoms in *1s* states. In rydberg energy units, Ry = $me^4/2\hbar^2$, we have

$$\gamma(Ry) = 2(1+\rho/a_0)\exp(-\rho/a_0), \quad \text{(A.12)}$$

where $a_0 = \hbar^2/me^2$. The overlap energy decreases exponentially with the separation in the case of 1s wavefunctions of hydrogen atoms [Kittel 1976].

The extension of this treatment on the electron energy band had been applied to the case of neutrons in lattice nuclei coupled with the super-nuclear interaction mediated by interstitial protons or deuterons [Kozima 2004a (Section 3), 2006 (Section 3.7)] and discussed further in the next section.

A.2a Fe 3*d* Bands Calculated by F. Stern

The use of the tight-binding approximation to calculate 3d electron bands in transition metals was performed by F. Stern for bcc Fe [Stern 1959]. He modified the tight-binding wavefunctions similar to the Wannier functions and succeeded to explain the cohesive energy of Fe. The calculation was repeated using the rather generalized method of APW (augmented plane wave method) by Wood and confirmed the Stern's result [Wood 1962].

Therefore, the calculations introduced in this and the previous subsections show that we can use the intuitive images of the free electron approximation and the tight-binding approximation for the electrons in solids.

A.2b Stoner-Wohlfarth Model of Ferromagnetism

The idea of tight-binding approximation to the lower-lying band structure was applied to 3*d* (Z = 21 – 30) bands in transition metals to explain appearance of magnetism depending on the atomic number Z. [Stoner 1924]

Electron bands can spontaneously split into up and down spins. This happens if the relative gain in exchange interaction (the interaction of electrons via the Pauli Exclusion Principle) is larger than the loss in kinetic energy (Fig. A6).

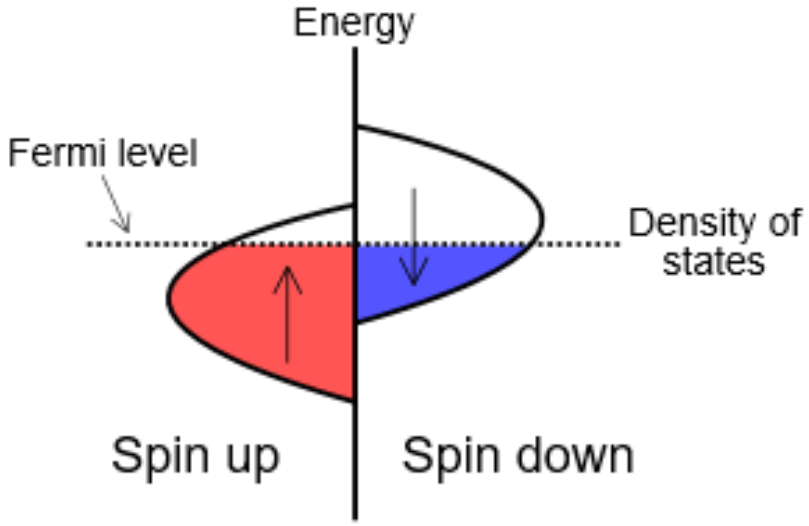

Fig. A6 A schematic band structure for the Stoner model of ferromagnetism. An exchange interaction has split the energy of states with different spins, and states near the Fermi level are spin-polarized (after “Edmund Clifton Stoner” from Wikipedia)

Rather realistic exposition of the density of state of 3*d* bands in transition metal Ni is shown in Fig. A7 after M. Wolf [Wolf 2005].

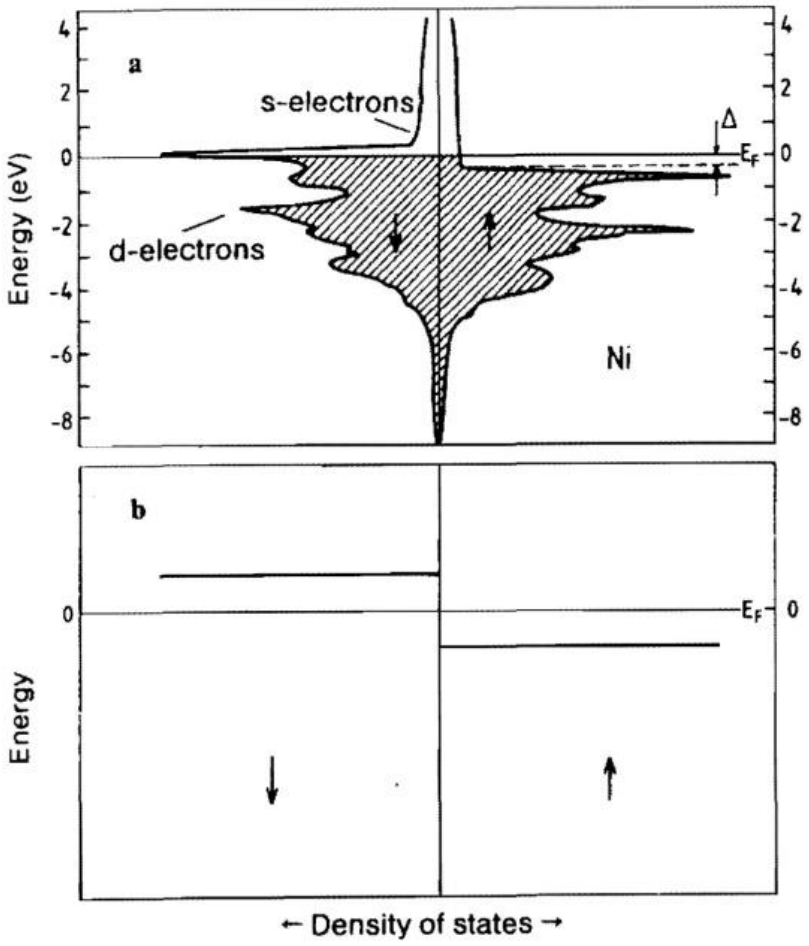

Fig. A7 Density of states by Stoner-Wohlfarth model of band ferromagnetism [Wolf 2005].

Filling the electrons of elements into the bands, we obtain the diagrams shown in Fig. A8 as a function of the valence electron number Z [Wolf 2005]. In the 3d-transition metal region (Z = 21 – 30), the Stoner parameter $I \cdot \underline{D}$ (ε_F) shows clearly the appearance of ferromagnetism at Fe, Co and Ni in accordance with experimental facts.

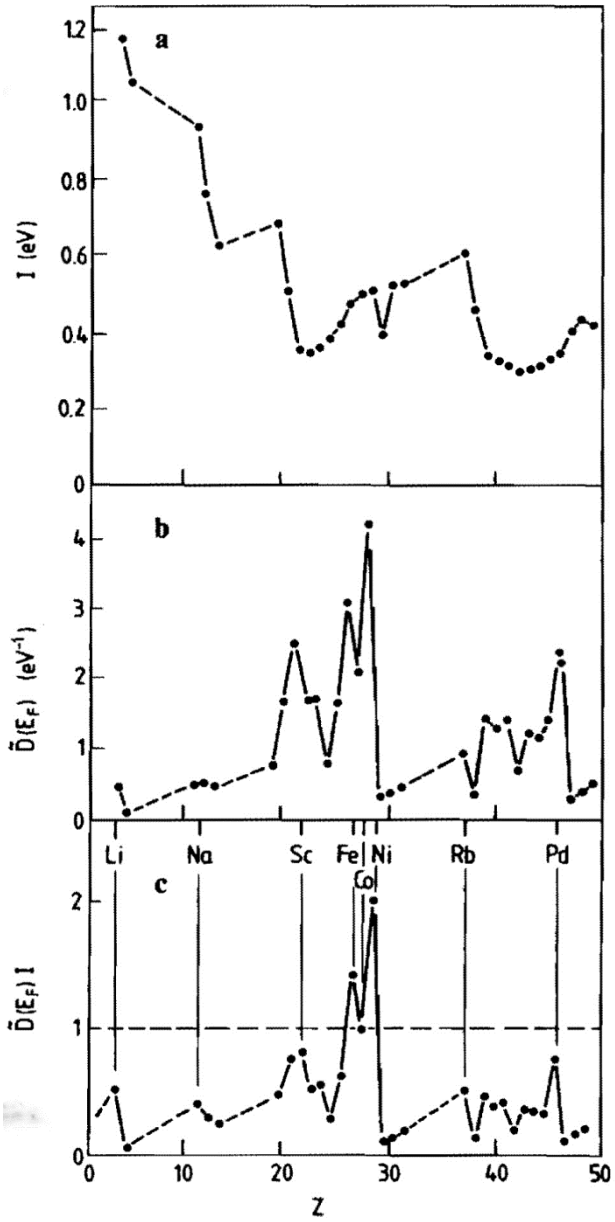

Fig. A8 Energy gain I (eV) from electron correlation, density of state per atom and spin orientation $\underline{D}$ (ε_F) at Fermi energy ε_F and $I \cdot \underline{D}$ (ε_F). Stoner criterion for the appearance of ferromagnetism is expressed as $I \cdot \underline{D}$ (ε_F) > 1 [Wolf 2005].

Acknowledgement

The authors would like to express their thanks to Dr. Y. Utsuno of JAEA (Japan Atomic Energy Agency) for his kind communications about recent development of the research on exotic nuclei.

References

[Blatt 1954] J.M. Blatt and V.F. Weisscopf, *Theoretical Nuclear Physics*, 2nd printing, John-Wiley & Sons, New York, 1954, ISBN-10: 0-471-08019-5.
[Bohr 1937] N. Bohr and K. Kalckar, Kg.. Danske Videnskab. Selskab, Mat-fys. Medd., **14**, 10 (1937).
[Bohr 1969] A. Bohr and B.R. Mottelson, *Nuclear Structure* I, Benjamin, New York, 1969.
[Callaway 1958] J. Callaway, "Electronic Wave Functions in Metallic Cesium," *Phys. Rev.*, **112,** 1061 – 1062 (1958).
[Caurier 2005] E. Caurier, G. Martínez-Pinedo, F. Nowacki, A. Poves and A. P. Zukeri, "The Shell Model as a Unified View of Nuclear Structure," *Rev. Mod. Phys*., **77**, 427 – 488 (2005).
[Cizewski 2010] J.A. Cizewski, K.L. Jones, R.L. Kozub, S.D. Pain and the ORRUBA/RIBENS Collaboration, "Single-particle Structure of Neutron-rich Nuclei," *Journal of Physics*: *Conference Series*, **239** (2010) 012007, doi:10.1088/1742-6596/239/1/012007.
[DOE 1989] *Cold Fusion Research*, November 1989－A Report of the Energy Research Advisory Board to the United States Department of Energy－, DOE/S-0071 (August, 1989) and DOE/S--0073, DE90, 005611. This report is posted at the *New Energy Times* website;
http://newenergytimes.com/v2/government/DOE/DOE.shtml
[DOE 2004] "*Report of the Review of Low Energy Nuclear Reactions.*" http://www.science.doe.gov/Sub/Newsroom/News_Releases/DOE-SC/2004/low_energy/CF_Final_120104.pdf. This report is posted at the *New Energy Times* website:
http://newenergytimes.com/v2/government/DOE2004/7Papers.shtml
[Fermi 1936] E. Fermi, *Ricerca Scientifica*, **7,** 13 (1936).
[Fleischmann 1989] M. Fleischmann, S. Pons and M. Hawkins, "Electrochemically induced Nuclear Fusion of Deuterium," *J. Electroanal. Chem.*, **261**, 301 – 308 (1989), ISSN: 1572-6657.
[Fukai 2005] Y. Fukai, *The Metal-Hydrogen System – Basic Bulk Properties –*, 2nd, Revised and Updated edition, Springer, Berlin, 2005, ISBN-10 3-540-00494-7.
[Golub 1990] R. Golub, D.J. Richardson and S.K. Lamoreaux, *Ultra-Cold Neutrons*, Adam Hilger, Bristol, 1990, ISBN 0-7503-0115-5.
[Hino 1998] M. Hino, N. Achiwa, S. Tasaki, T. Ebisawa, T. Akiyoshi and T. Kawai, "Observation of Quasi-bound States of Neutron in Fabry-Perot Magnetic Thin Film Resonator using Larmor Precession," *Physica B*, Vol. **241 – 243**, pp. 1083 – 1085 (1998). The revised and enlarged version of this paper is published in the following

journal: M. Hino, N. Achiwa, S. Tasaki, T. Ebisawa, T. Kawai and D. Yamazaki, T. Kawai and D. Yamazaki, "Measurement of Spin-precession Angles of Resonant Tunneling Neutrons," *Phys. Rev.*, **A61**, 013607-1 – 8 (2000).

[JAERI 1997] *JAERI-Data/Code* 97-003 (Part I) "Curves and Tables of Neutron Cross Sections" in JENDL-3.2 Part I (Z = 1 – 50) February 1997.

[Jones 1989] S.E. Jones, E.P. Palmer, J.B. Czirr, D.L. Decker, G.L. Jensen, J.M. Thorne, S.F. Tayler and J. Rafelski, "Observation of Cold Nuclear Fusion in Condensed Matter," *Nature*, **338**, 737 – 740 (1989).

[Kittel 1976] C. Kittel, *Introduction to Solid State Physics*, 5th Edition, John Wiley & Sons, New York, 1976, ISBN 0-471-49024-5.

[Kozima 1961] H. Kozima, "Electron Wave Functions in Metallic Sodium," *Technical Report of ISSP*, **B2**, 1 – 3 (1961).

[Kozima 1994] H. Kozima, "Trapped Neutron Catalyzed Fusion of Deuterons and Protons in Inhomogeneous Solids," *Trans. Fusion Technol.*, **26**, 508 – 515 (1994). ISSN 0748-1896.

[Kozima 1998a] H. Kozima, *Discovery of the Cold Fusion Phenomenon* (Ohtake Shuppan Inc., 1998), ISBN 4-87186-044-2.

[Kozima 1998b] H. Kozima, "Neutron Band in Solids," *J. Phys. Soc. Japan*, **67**, 3310 – 3311 (1998), ISSN: 0031-9015. And also, *Elemental Energy* (*Cold Fusion*) **28**, 30 (1998), ISSN 1074-5610.

[Kozima 2004a] H. Kozima, "Quantum Physics of Cold Fusion Phenomenon," in *Development of Quantum Physics Researches – 2004*, pp. 167 – 196 (F. Columbus and V. Krasnoholovets, ed.), Nova Science Publishers Inc., New York, ISBN 1-59454-003-9.

[Kozima 2004b] H. Kozima, "Solid State-Nuclear Physics of Cold Fusion Phenomenon," *Reports of CFRL (Cold Fusion Research Laboratory)* **2-1**, 1 – 35 (2004);
http://www.geocities.jp/hjrfq930/Papers/paperr/paperr.html

[Kozima 2005] H. Kozima, "CF-Matter and the Cold Fusion Phenomenon," *Proc. ICCF10*, pp. 919 – 928 (2005), ISBN 981-256-564-7.

[Kozima 2006] H. Kozima, *The Science of the Cold Fusion Phenomenon*, Elsevier Science, 2006. ISBN-10: 0-08-045110-1.

[Kozima 2008] H. Kozima, "Physics of the Cold Fusion Phenomenon," *Proc. ICCF13*, pp. 690 – 703 (2008), ISBN 978-5-93271-428-7.

[Kozima 2009a] H. Kozima, "Non-localized Proton/Deuteron Wavefunctions and Neutron Bands in Transition-metal Hydrides/Deuterides," *Proc. JCF9*, pp. 84 – 93 (2009), ISSN 2187-2260. And also *Reports of CFRL* (*Cold Fusion Research*

Laboratory) 9-3, pp. 1 – 10 (October, 2009);
http://www.geocities.jp/hjrfq930/Papers/paperr/paperr.html
[Kozima 2009b] H. Kozima, "On the Methodology of the Cold Fusion Research," *Reports of CFRL* (*Cold Fusion Research Laboratory*), **9-5**, pp. 1 – 39 (November, 2009),
http://www.geocities.jp/hjrfq930/Papers/paperr/paperr.html
[Kozima 2010] H. Kozima and H. Date, "Nuclear Transmutations in Polyethylene (XLPE) Films and Water," *Proc. ICCF14* (August 10 – 15, 2008, Washington D.C., U.S.A.) pp. 618 – 622 (2010), ISBN: 978-0-578-06694-3 and also *Reports of CFRL*, **8-2**, pp. 1 – 16 (August, 2008);
http://www.geocities.jp/hjrfq930/Papers/paperr/paperr.html
[Kozima 2011] H. Kozima, "Three Laws in the Cold Fusion Phenomenon and Their Physical Meaning," *Proc. JCF12*, pp. 101 – 114 (2012), ISSN 2187-2260. And also *Reports of CFRL* (*Cold Fusion Research Laboratory*) 11-6, 1 – 14 (April, 2011);
http://www.geocities.jp/hjrfq930/Papers/paperr/paperr.html
[Kozima 2012] H. Kozima, "Cold Fusion Phenomenon in Open, Non- equilibrium, Multi-component Systems," *Reports of CFRL* (*Cold Fusion Research Laboratory*), 12-1, 1 – 14 (January, 2012);
http://www.geocities.jp/hjrfq930/Papers/paperr/paperr.html
[Kozima 2013] H. Kozima, "Cold Fusion Phenomenon in Open, Nonequilibrium, Multi-component Systems – Self-organization of Optimum Structure," *Proc. JCF13* **13-19**, pp. 134 – 157 (2013), ISSN 2187-2260. And also *Reports of CFRL* (*Cold Fusion Research Laboratory*), 13-3, 1 – 24 (March, 2013);
http://www.geocities.jp/hjrfq930/Papers/paperr/paperr.html
[Kozima 2014a] H. Kozima, "The Cold Fusion Phenomenon – What is It?" *Proc. JCF14*: **14-16**, pp. 203 – 230 (2014), ISSN 2187-2260;
http://jcfrs.org/file/jcf14-proceedings.pdf
And also *Reports of CFRL* (*Cold Fusion Research Laboratory*) 14-4, 1 – 29 (March, 2014); http://www.geocities.jp/hjrfq930/Papers/paperr/paperr.html
[Kozima 2014b] H. Kozima and K. Kaki, "Atomic Nucleus and Neutron — Nuclear Physics Revisited with the Viewpoint of the Cold Fusion Phenomenon" *Proc. JCF14*, **14-5**, pp. 47 - 76 (2014). ISSN 2187-2260;
http://jcfrs.org/file/jcf14-proceedings.pdf
And also *Reports of CFRL* (*Cold Fusion Research Laboratory*) **14-1**, 1 – 34 (March, 2014); http://www.geocities.jp/hjrfq930/Papers/paperr/paperr.html
[Kozima 2014c] H. Kozima, "Nuclear Transmutations (NTs) in Cold Fusion

Phenomenon (CFP) and Nuclear Physics," *Proc. JCF14*, **14-15**, pp. 168 - 202 (2014). ISSN 2187-2260.
http://jcfrs.org/file/jcf14-proceedings.pdf
[Kozima 2015] H. Kozima, *From the History of CF Research* (2015);
http://www.geocities.jp/hjrfq930/Papers/paperf/paperf.html
[Morfouace 2014] P. Morfouace and 19 others, "Single-particle Strength in Neutron-rich ^{69}Cu," *Acta Physica Polonica*, **B45**, 243 – 248 (2014).
[Negele 1973] J.W. Negele and D. Vautherin, "Neutron Star Matter at Sub-nuclear Densities," *Nuclear Physics*, A207, 298 – 320 (1973), ISSN: 0375-9474.
[Sahin 2015] E. Sahin and 73 others, "Shell Evolution Beyond N = 40: ^{69,71,73}Cu," *Phys. Rev*., **C91**, 0343021-1 – 9 (2015).
[Scheckenhofer 1977] H. Scheckenhofer and A. Steyerl, "Diffraction and Mirror Reflection of Ultracold Neutrons," *Phys. Rev. Lett*., 39, 1310 – 1312 (1977).
[Sharp 2013] D.K. Sharp and 19 others, "Neutron Single-particle Strength outside the N=50 Core," *Phys. Rev.,* **C 87,** 014312-1 – 11 (2013).
[Shull 1947] C.G. Shull and E.O. Wollan, "The Diffraction of Neutrons by Crystalline Powders", Oak Ridge National Laboratory (ORNL), United States Department of Energy (through predecessor agency the Atomic Energy Commission), (April 28, 1947).
[Shull 1956] C. G. Shull and E O Wollan: Application of Neutron Diffraction to Solid State Problems, *Solid State Physics*, Vol.2, Academic Press, New York, p.138 – 217, 1956, Library of Congress Catalog Card Number: 55-12299.
[Steinhauser 1980] K.A. Steinhauser, A. Steyerl, H. Scheckenhofer, and S.S. Malik, "Observation of Quasibound States of the Neutron in Matter," *Phys. Rev. Lett*., **44**, 1306 – 1309 (1980).
[Stern 1959] F. Stern, "Calculation of the Cohesive Energy of Metallic Iron," *Phys. Rev.*, 116, 1399 – 1417 (1959).
[Stoner 1924] E.C. Stoner, "The Distribution of Electrons among Atomic Levels," *Philosophical Magazine* (6th series) **48**, pp. 719–736 (1924).
[Stroberg 2014] S.R. Stroberg and 18 others, "Single-particle Structure of Silicon Isotopes Approaching Si42," *Phys. Rev.,* **C 90,** 034301 (2014).
[Stroberg 2015] S.R. Stroberg and 18 others, "Neutron Single-particle Strength in Silicon Isotopes: Constraining the Driving Forces of Shell Evolution," arXiv:1504.02329v1 [nucl-ex] 9 Apr 2015..
[Utsuno 2014] Y. Utsuno, T. Otsuka, N. Shimizu, M. Honma, T. Mizusaki, Y. Tsunoda and T. Abe, "Recent Shell-Model Results for Exotic Nuclei," EPJ Web of Conferences, **66,** 02106 (2014). DOI: 10.1051/ epjconf/ 20146602106.

[Wood 1962] J.H. Wood, “Energy Bands in Iron via the Augmented Plane Wave Method,” *Phys. Rev.*, **126**, 517 – 527 (1962).